# Conclusive Identification of Quantum Channels via Monogamy of Quantum Correlations

Asutosh Kumar[1,2], Sudipto Singha Roy[1,2], Amit Kumar Pal[1,2], R. Prabhu[1,2,3], Aditi Sen(De)[1,2], and Ujjwal Sen[1,2]

[1]*Harish-Chandra Research Institute, Chhatnag Road, Jhunsi, Allahabad 211019, India*
[2]*Homi Bhabha National Institute, Training School Complex, Anushaktinagar, Mumbai 400094, India*
[3]*Department of Physics, Indian Institute of Technology Patna, Bihta 801103, Bihar, India*

We investigate the action of local and global noise on monogamy of quantum correlations, when monogamy scores are considered as observables, and three-qubit systems are subjected to global noise and various local noisy channels, namely, amplitude-damping, phase-damping, and depolarizing channels. We show that the dynamics of monogamy scores corresponding to negativity and quantum discord, in the case of generalized W states, as inputs to the noisy channels, can exhibit non-monotonic dynamics with respect to increasing noise parameter, which is in contrast to the monotonic decay of monogamy scores when generalized Greenberger-Horne-Zeilinger states are exposed to noise. We quantify the persistence of monogamy against noise via a characteristic value of the noise parameter, and show that depolarizing noise destroys monogamy of quantum correlation faster compared to other noisy channels. We demonstrate that the negativity monogamy score is more robust than the quantum discord monogamy score, when the noise is of the phase-damping type. We also investigate the variation of monogamy with increasing noise for arbitrary three-qubit pure states as inputs. Finally, depending on these results, we propose a two-step protocol, which can conclusively identify the type of noise applied to the quantum system, by using generalized Greenberger-Horne-Zeilinger and generalized W states as resource states. We discuss a possible generalization of the results to higher number of parties.

## I. INTRODUCTION

An important characterization of a composite quantum system is by the correlations, both classical and quantum, between its constituting parts. Quantum information theory provides a collection of measures of quantum correlations [1–3], which can broadly be categorized into two classes. One is the "entanglement-separability" class, encompassing various measures of quantum entanglement in both bipartite and multipartite domain [1]. The other is the information-theoretic regime [2, 3], consisting of quantum correlations such as quantum discord [4], and various "discord-like" measures [5, 6], that quantify quantum correlations beyond entanglement. Both entanglement as well as information theoretic quantum correlation measures have been proposed to be resources for several quantum protocols [7–18], and have been observed successfully in the laboratory [19, 20]. However, quantum correlations, especially entanglement, have been found to be fragile under decoherence [21]. Naturally, due to their immense importance in quantum information processing tasks, investigating the behavior of quantum correlations under various kinds of environmental noise has been a topic of utmost importance in quantum information theory.

Most of the available literature that deals with decoherence of quantum correlations consider bipartite quantum correlation measures due to their relative computational simplicity [22, 23, 25–30]. It has been shown that the bipartite entanglement measures tend to decay rapidly with increasing noise, and vanish when a threshold noise level is crossed. This phenomena is known as "entanglement sudden death", and has been studied extensively in the case of bipartite systems under different types of environments [22, 23]. In stark contrast to this behavior, information theoretic measures, namely, quantum discord, quantum work deficit, and several geometric measures, have been found to undergo an asymptotic decay with increasing noise strength [24–27], indicating a higher robustness against noise than that of entanglement. It has also been shown that special two- as well as multiqubit mixed quantum states can be engineered for which "discord-like" quantum correlations may remain frozen

over a finite range of noise strength [28, 29], while the entanglement measures for those states exhibit no such property (cf. [30]). Although behavior of bipartite quantum correlations under decoherence is a well-investigated topic, similar studies in the multipartite scenario [31] are limited due to the lack of computable measures of quantum correlations for mixed multipartite states.

Recent developments on the monogamy relation of quantum correlations [32–36] have provided an effective tool to investigate the multipartite nature of quantumness present in a composite quantum system. Qualitatively, monogamy of a quantum correlation measure corresponding to a multipartite state is the property that allows a chosen party to share only limited amount of quantum correlation with all the other parties except one, to which it is highly quantum correlated. Interestingly, such monogamy constraints can be quantified via the "monogamy score" [37], leading to multipartite quantum correlation measures that use bipartite measures of quantum correlations, thereby reducing the difficulty in the computation of the measures for multipartite states. The monogamy property of quantum correlations has been shown to be important in several aspects in quantum mechanics and quantum information, like foundations of quantum mechanics [38], quantum cryptography [39], teleportation [40], quantum dense coding [41], quantum steering [42], many-body physics [43], and black-hole information theory [44]. Experimental investigation of this property has also been initiated [45]. Therefore, it has become important to investigate the behavior of the monogamy property of quantum correlations when the system is subjected to noisy environments.

This paper has two different objectives that are complementary to each other. In one, we study the dynamics of monogamy of quantum correlations. As measures of quantum correlations, we use the monogamy scores of two bipartite quantum correlation measures, namely, the negativity [46, 47], a measure of bipartite entanglement, and quantum discord [4, 48], a quantum correlation measure from the information-theoretic domain. We choose a global noise, and three local noisy channels, namely, the amplitude-damping (AD), the phase-damping (PD), and the

depolarizing (DP) channels as different models of environmental noise [21, 24, 49–53]. We demonstrate how the dynamics of monogamy, in the case of three-qubit systems, exhibit qualitatively different behavior depending on whether the input quantum state is chosen from the family of generalized Greenberger-Horne-Zeilinger (gGHZ) state [54], or the generalized W (gW) states [55–57], which are not equivalent under stochastic local operations and classical communication (SLOCC). More specifically, we show that monogamy scores of negativity as well as quantum discord exhibit a monotonic decay with respect to the corresponding noise parameter, when gGHZ state is subjected to these noise models, while there exist non-monotonic dynamics when the input state is the gW state. We also investigate the trends of monogamy scores against noise, when arbitrary three-qubit pure states belonging to the two inequivalent SLOCC classes of three-qubit pure states, namely, the GHZ and the W classes [57], are chosen as inputs. Moreover, we introduce a concept called the "dynamics terminal", which quantify the durability of quantum correlation measures under decoherence, and show that it can distinguish between different quantum correlation measures as well as different types of noise. The study also reveals that for the PD channel, the negativity monogamy score can exhibit a more robust behavior against noise strength than that observed for the monogamy score of quantum discord, which we call the "discord monogamy score".

Besides characterizing the dynamical features of quantum correlations under decoherence, it is also interesting to address the reverse question as to whether the modes of environmental noise can be identified by using the properties of quantum correlations. Although a few studies have been motivated by similar goal [58], the literature regarding this issue is extremely limited. While most of the studies have tried to distinguish different types of noise by the different dynamical behavior of different quantum correlations, concrete protocol to conclusively identify the type of noise to which the quantum state is exposed is yet to be introduced. As the second objective of this paper, we use the highly entangled gGHZ and any gW states as resources, and design a two-step protocol involving the monogamy relations of negativity and quantum discord to conclusively distinguish the type of noise applied to the quantum state, where the noise models include a global noise, and several local channels, namely, AD, PD, and DP channels.

The paper is organized as follows. In Sec. II, we discuss the dynamical behavior of the negativity and discord monogamy scores, when the gGHZ and the gW states are subjected to different types of noise. The behavior of monogamy against noise, when arbitrary three-qubit pure states are considered as input, is also studied in this section. In Sec. III, the two-step channel discrimination protocol with monogamy scores is presented. Sec. IV presents the concluding remarks.

## II. MONOGAMY OF QUANTUM CORRELATIONS UNDER DECOHERENCE

In this section, we investigate the behavior of monogamy scores corresponding to negativity and quantum discord for three-qubit quantum states under the influence of global as well as local noise. Brief descriptions of the quantum corre-
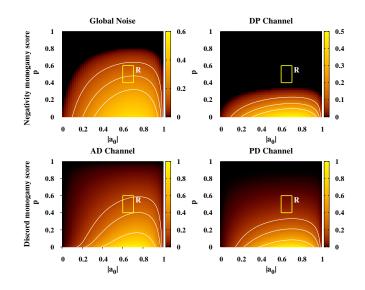


FIG. 1. (Color online.) (Top panels) Variations of $\delta_{\mathcal{N}}$ as functions of the noise parameter, $p$, and the state parameter, $|a_0|$, when gGHZ states are subjected to global noise (left) and DP channel (right). (Bottom panels) Variations of $\delta_{\mathcal{D}}$ as functions of the noise parameter, $p$, and the state parameter, $|a_0|$, when gGHZ states are subjected to AD channel (left) and PD channel (right). The absolute value of the other state parameter, $|a_1|$, is determined by normalization. The solid lines in the plots are the contours obtained by joining the points corresponding to a fixed value of either $\delta_{\mathcal{N}}$, or $\delta_{\mathcal{D}}$. In the case of $\delta_{\mathcal{N}}$, the lines, from low to high values of $p$, correspond to $\delta_{\mathcal{N}} = 0.3, 0.2$, and $0.1$, while for $\delta_{\mathcal{D}}$, they represent the contours of $\delta_{\mathcal{D}} = 0.6, 0.3$, and $0.15$. The regions marked by "**R**", and enclosed by the boxes are defined by the ranges $0.65 \le |a_0| \le 0.7071$, and $0.4 \le p \le 0.6$. The implications of these ranges of values are discussed in Sec. III. All the quantities plotted are dimensionless, except for $\delta_{\mathcal{D}}$, which is in bits.

lation measures, namely, negativity and quantum discord, and monogamy of quantum correlations can be found in [59]. Discussions on different types of noise considered in this paper are provided in [59]. Before considering arbitrary three-qubit pure states, we examine the generalized GHZ (gGHZ), and the generalized W (gW) states as the input states to various types of noise.

### A. Generalized GHZ states

The generalized GHZ state, shared between three qubits, 1, 2, and 3, reads as

$$|\Psi_3\rangle = a_0|000\rangle + a_1|111\rangle, \tag{1}$$

where $a_0$ and $a_1$ are the complex parameters satisfying $|a_0|^2 + |a_1|^2 = 1$. In this paper, we consider qubit 1 as the nodal observer while computing monogamy scores for negativity ($\delta_{\mathcal{N}}$), and quantum discord ($\delta_{\mathcal{D}}$). Note that the monogamy scores for the gGHZ state, in the noiseless scenario, is always positive for all quantum correlation measures including negativity and quantum discord. This is due to the fact that the two-qubit reduced density matrix $\rho_{12} = \rho_{13} = |a_0|^2|00\rangle\langle00| + |a_1|^2|11\rangle\langle11|$,

obtained from the gGHZ state, is a classically correlated two-qubit state having vanishing quantum correlations, while the state $|\Psi_3\rangle$ in the $1:23$ bipartition always has a non-zero value of quantum correlation for $a_0, a_1 \neq 0$. Even for the noise parameter $p \neq 0$, $\delta_{\mathcal{N}}$ and $\delta_D$ are given by $\delta_{\mathcal{N}} = \mathcal{N}\left(\rho_{1:23}^{\text{gGHZ}}\right)$ and $\delta_{\mathcal{D}} = \mathcal{D}\left(\rho_{1:23}^{\text{gGHZ}}\right)$ respectively, when the gGHZ state is subjected to the four types of noise considered in this paper (see [59]). Hence, both negativity and quantum discord are always monogamous in the present scenario, which can be applied to discriminate channels, as we shall see in Sec. III. Note that the entire discussion also holds for gGHZ states of an arbitrary number of parties subjected to the different types of local and global noise considered here.

The above discussion helps one to determine analytical expressions for negativity monogamy score as a function of the noise parameter in the case of different types of noise [59]. On the other hand, analytically determining the discord monogamy score, $\delta_{\mathcal{D}}$, for all the types of noise, is in general hard due to the optimization required to compute quantum discord for $\rho^{\text{gGHZ}}$ in the $1:23$ split [60]. So far, analytical determination of quantum discord has been possible only for very restricted class of mixed states [61, 62]. Hence, we employ numerical optimization over the real parameters $(\theta, \phi)$ of measurement involved in the definition of quantum discord. The behavior of the monogamy scores corresponding to negativity and quantum discord for different types of noise are depicted in Fig. 1, where the top panels are for $\delta_{\mathcal{N}}$, and the bottom panels correspond to $\delta_{\mathcal{D}}$. For all the noise models considered in this paper, $\delta_{\mathcal{N}}$ and $\delta_{\mathcal{D}}$ monotonically decreases with increasing values of $p$ for a fixed value of $|a_0|$, and vanishes when noise is considerably high, as can be clearly seen from the figures. The regions (in Fig. 1) marked by "**R**", and enclosed by the boxes are defined by the parameter ranges $0.65 \leq |a_0| \leq 0.7071$, and $0.4 \leq p \leq 0.6$, respectively. Note that in the marked areas, $\delta_{\mathcal{N}} > 0$ for global noise, while $\delta_{\mathcal{N}} = 0$ under DP channel. On the other hand, in the region **R**, $\delta_{\mathcal{D}} > 0$ for both AD and PD channels. The implications of these values are discussed in Sec. III.

### B. Generalized W states

Let us now move to the monogamy scores of negativity and quantum discord for the gW state, given by

$$|\Phi_3\rangle = a_0|001\rangle + a_1|010\rangle + a_2|100\rangle, \quad (2)$$

where $a_0, a_1$ and $a_2$ are complex numbers, satisfying $|a_0|^2 + |a_1|^2 + |a_2|^2 = 1$. Unlike the gGHZ state, the reduced states obtained from the gW states with, as well as without, noise, are quantum correlated states, possessing non-zero values of entanglement as well as quantum discord. This makes the evaluation of monogamy scores, for both negativity and quantum discord, involved, in comparison to the case of the gGHZ state. However, analytical expressions for $\delta_{\mathcal{N}}$ can be determined for the global as well as the different types of local noise [59]. On the other hand, the computation of $\delta_{\mathcal{D}}$, in case of the gW states under noise, requires more numerical resources than that in the case of the gGHZ states, since both $\mathcal{D}\left(\rho_{12}^{\text{gW}}\right)$ and $\mathcal{D}\left(\rho_{13}^{\text{gW}}\right)$ do not vanish

for almost all $p$. In the present case, $\delta_{\mathcal{D}}$ can be written as

$$\delta_{\mathcal{D}} = S - S(\rho_1^{\text{gW}}) - S_c, \quad (3)$$

where $S = S(\rho_{12}^{\text{gW}}) + S(\rho_{13}^{\text{gW}}) - S(\rho^{\text{gW}})$, and $S_c = S(\rho_{2|1}^{\text{gW}}) + S(\rho_{3|1}^{\text{gW}}) - S(\rho_{23|1}^{\text{gW}})$. The determination of $\delta_{\mathcal{D}}$ for a single three-qubit state requires, in principle, three separate optimizations for the terms in $S_c$. However, information acquired via numerical analysis using constrained optimization [29, 63–65] may result in considerable reduction of the computational complexity (see [59] for a discussion).

**Behavior of monogamy under moderate noise.** Let us now quantitatively study the behavior of monogamy scores, $\delta_{\mathcal{N}}$ and $\delta_{\mathcal{D}}$, of the gW states for a fixed noise parameter. We determine the fractions of the set of $\rho^{\text{gW}}$, for which the monogamy score corresponding to the chosen quantum correlation measure is strictly greater than, equal to, and strictly less than zero. We study the variation of these fractions with the change in values of the noise parameter for the specified type of noise. The variations of the three different fractions, as described above, with respect to $p$, are depicted in Fig. 2. Let us now investigate the effect of moderate noise on the monogamy scores. In the present study, we choose a range of $p$ given by $0.4 \leq p \leq 0.6$ (marked by the shaded regions in the panels in Fig. 2), which is moderate in comparison to the lower and upper bounds of $p$. From Fig. 2, it is clear that for moderate values of $p$ (viz. $0.4 \leq p \leq 0.6$), in the case of global noise as well as the AD channel, most of the states have $\delta_{\mathcal{N}} > 0$, while for the DP channel, $\delta_{\mathcal{N}} = 0$ for $100\%$ of the states. Remarkably, for the PD channel, all the states have $\delta_{\mathcal{N}} > 0$ when the noise parameter is in the moderate range.

The situation is different for discord monogamy score. It is found that $\delta_{\mathcal{D}} \geq 0$ for almost the entire range of moderate values of $p$, when gW states are subjected to global noise. In the case of the AD channel, $\delta_{\mathcal{D}} < 0$ for the entire range $0.4 \leq p \leq 0.6$. In this scenario, $\delta_{\mathcal{D}} < 0$ for the entire range of $p$, except only at $p = 1$, the fully decohered states. Also, for the PD channel, $\delta_{\mathcal{D}} < 0$ for moderate $p$ except when $p \approx 0.6$. However, in the case of the DP channel, $\delta_{\mathcal{D}} \geq 0$ for $0.4 \leq p \leq 0.6$. Hence it is clear that the monogamy of negativity behaves differently than the monogamy of quantum discord, in the case of global noise, and local channels considered in this paper. These results are of prime importance to our goal of channel discrimination, which will be discussed in Sec. III.

**Types of dynamics.** In case of the gW state subjected to global or local noise, the set of different types of dynamics that $\delta_{\mathcal{N}}$ and $\delta_{\mathcal{D}}$ undergo is far richer compared to that for gGHZ states. While only monotonic decay of $\delta_{\mathcal{N}}$ and $\delta_{\mathcal{D}}$ with increasing $p$ is found in the latter case, non-monotonic dynamics of monogamy scores emerges in the former (see [59] for an example). Now we catalog four "typical" dynamics profiles observed for both $\delta_{\mathcal{N}}$ and $\delta_{\mathcal{D}}$ for global noise as well as for AD, PD, and DP local channels. **a.** In the first profile, $\delta_{\mathcal{Q}}(p = 0) \geq 0$, and $\delta_{\mathcal{Q}}(p)$ goes to zero non-monotonically as $p \to 1$. **b.** For the second one, $\delta_{\mathcal{Q}}(p)$ monotonically goes to zero when $p$ increases, with $\delta_{\mathcal{Q}}(p = 0) \geq 0$. **c.** In contrast to the first two profiles, $\delta_{\mathcal{Q}}(p = 0) < 0$ for the third profile. With an increase of $p$, $\delta_{\mathcal{Q}}$ vanishes non-monotonically. **d.** Similar to the third profile, the fourth and the final profile starts with a non-monogamous scenario ($\delta_{\mathcal{Q}}(p = 0) < 0$). However, with increasing $p$, $\delta_{\mathcal{Q}}(p)$
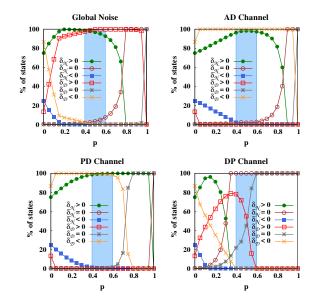
FIG. 2. (Color online.) Variations of the percentages of states for which $\delta_{\mathcal{N}}$ and $\delta_{\mathcal{D}}$ are greater than, equal to, and less than zero, for different types of noise considered in this paper. The range of moderate noise, given by $0.4 \leq p \leq 0.6$, is shown by the shaded region in each figure. All quantities plotted are dimensionless.
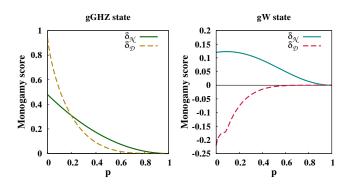


FIG. 3. (Color online.) Dynamics profiles of $\delta_{\mathcal{N}}$ (solid line) and $\delta_{\mathcal{D}}$ (dashed line) in the case of the input gGHZ state given by $|a_0| = 0.7$ (left panel), and the input gW state given by $a_0 = -0.287 - 0.552i$, and $a_1 = 0.637 + 0.23i$ (right panel). In both the cases, $\delta_{\mathcal{N}}$ remains positive for higher values of $p$ ($p \geq 0.6$), while $\delta_{\mathcal{D}}$ vanishes. Note that for the gW states considered here, $\delta_{\mathcal{N}}$ exhibits a type-**a** dynamics, while that of $\delta_{\mathcal{D}}$ is of type-**c**. All the quantities plotted are dimensionless, except for $\delta_{\mathcal{D}}$, which is in bits.

goes to zero monotonically as $p \to 1$. Fig. 3 depicts two typical profiles of type-**(a)** and type-**(c)** dynamics for $\delta_{\mathcal{N}}$ and $\delta_{\mathcal{D}}$, respectively. A statistics on the occurrences of the four types of dynamics in the case of gW states is given in [59].

**Dynamics terminal.** So far, we have qualitatively discussed and characterized the dynamics of $\delta_{\mathcal{N}}$ and $\delta_{\mathcal{D}}$ under the application of global and local noise to the gW state. It is observed as well as intuitively clear that the persistence of the monogamy scores, when subjected to noise, must be different for different types of noise considered in this paper. To analyze this quantitatively, for a given state, $\rho$, we define the "dynamics terminal", $p_t$, which is given by the value of the noise parameter, $p$, at which the

| Noise | $\langle p_t \rangle$ for $\delta_{\mathcal{N}}$ | $\langle p_t \rangle$ for $\delta_{\mathcal{D}}$ |
|---|---|---|
| Global | 0.733 | 0.947 |
| AD | 0.667 | 0.986 |
| PD | 0.940 | 0.584 |
| DP | 0.274 | 0.331 |

TABLE I. The average values of dynamics terminal, $\langle p_t \rangle$, for $\delta_{\mathcal{N}}$ and $\delta_{\mathcal{D}}$, when gW states are subjected to various kinds of noise. The profiles of the probability density function, $P(p_t)$, corresponding to different types of noise, for both $\delta_{\mathcal{N}}$ and $\delta_{\mathcal{D}}$, are given in [59].

monogamy score vanishes, and remains so for $p_t \leq p \leq 1$. The value of $p_t$ is characteristic to the input state, $|\Phi\rangle$, and the type of noise applied to it. A high value of $p_t$ implies a high persistence of the monogamy score for the state $|\Phi\rangle$ against the particular type of noise applied to it. It is clear that for gW states as the input states, $p_t$ may assume a range of values since the dynamics terminal will clearly have different values for different input gW states, when the type of noise is fixed. However, for a specific type of noise, the average value of $p_t$, denoted by $\langle p_t \rangle$, and defined by

$$\langle p_t \rangle = \int_0^1 p_t P(p_t) dp_t, \tag{4}$$

provides a scale for the "high" values of the noise parameter. Here, $P(p_t)$ is the normalized probability density function (PDF) such that $P(p_t)dp_t$ provides the probability that for an arbitrary three-qubit gW state under the fixed type of noise, the value of $p_t$ lies between $p_t$ and $p_t + dp_t$. Note that the full range of the allowed values of $p_t$ is given by $0 \leq p_t \leq 1$, which follows from the definition of the noise parameter. The values of $\langle p_t \rangle$ corresponding to $\delta_{\mathcal{N}}$ and $\delta_{\mathcal{D}}$, calculated from Eq. (4), for global noise, AD channel, PD channel, and DP channel are given in Table I (see [59] for the numerical details).

**Note.** Due to the extensive numerical effort required for determining the values of $\mathcal{D}(\rho_{1:23}^{\text{gW}})$, $\mathcal{D}(\rho_{12}^{\text{gW}})$, and $\mathcal{D}(\rho_{13}^{\text{gW}})$ in computing $\delta_{\mathcal{D}}$ when $p > 0$, we employ the constrained optimization technique [29, 59, 63–65] to obtain several important statistics reported in [59]. However, the error in the various statistics obtained for different channels, due to this approximation, is insignificant, and does not change the qualitative aspects of the results. Note that in all the occasions in this paper, where actual value of $\delta_{\mathcal{D}}$ has been plotted, or reported, exact optimization has been carried out using numerical techniques.

**Robustness of negativity monogamy score.** As already mentioned in the Introduction, in the bipartite domain, it has been observed that quantum discord vanishes asymptotically with increasing noise strength, $p$, when quantum states are exposed to local noise. On the other hand, entanglement measures undergo a "sudden death" at a finite value of $p$ under similar noise, indicating a more fragile behavior than quantum discord. Interestingly, an opposite trend is observed when monogamy of quantum correlations are subjected to local noisy channels. The variation of $\delta_{\mathcal{N}}$ and $\delta_{\mathcal{D}}$ with $|a_0|$ and $p$ in the case of PD channels with gGHZ states as input states (Fig. 1) indicates that there exists gGHZ states for which $\delta_{\mathcal{N}}$ persists longer than $\delta_{\mathcal{D}}$ for higher values of the noise parameter, $p$ ($p \geq 0.8$). Our analysis also shows that the value of $\langle p_t \rangle$ for negativity monogamy score, in the case of the DP channel, is much larger compared to that of

the discord monogamy score. Also, Fig. 2 indicates that for higher values of $p$ ($0.6 \leq p \leq 0.9$), 100% of gW states have $\delta_{\mathcal{N}} > 0$ when the noise is of PD type. Note that for all such states, $\delta_{\mathcal{D}} \leq 0$. This implies that there is a finite probability of finding gW states which, when subjected to PD channel, will evolve into a state $\rho^{\text{gW}}$ with $\delta_{\mathcal{N}} > 0$, but $\delta_{\mathcal{D}} = 0$.

We present two specific examples to establish such observations. Our first example is the gGHZ states represented by $|a_0| = 0.6$, while the second example is the gW states given in Eq. (2) with $a_0 = -0.287 - 0.552i$, and $a_1 = 0.637 + 0.23i$. The behavior of $\delta_{\mathcal{N}}$ and $\delta_{\mathcal{D}}$ against $p$ are plotted in Fig. 3, where the quantum discord components of $\delta_{\mathcal{D}}$ are computed via exact numerical optimization. It is clear from the figure that in both the cases, $\delta_{\mathcal{N}}$ persists longer than $\delta_{\mathcal{D}}$ at higher end of noise parameter. One must note here that the quantum discord components of $\delta_{\mathcal{D}}$ cancel each other at higher noise, while being individually non-zero. Hence the observation of $\delta_{\mathcal{N}} > 0$ in situations where $\delta_{\mathcal{D}} = 0$ is consistent with the fact that entanglement measures vanish for zero discordant states in bipartite systems. Therefore, it is evident that negativity monogamy score, in the presence of PD noise, exhibits a more robust behavior compared to that of the discord monogamy score. This is in contrast to the usual observation for bipartite quantum discord and entanglement measures.

Hitherto, we have investigated gGHZ and gW states, for which the effects of various noisy channels on monogamy scores can be addressed analytically up to certain extent. To complete the investigation for three-qubit states as input, we now consider the two mutually exclusive and exhaustive classes of three-qubit states, viz., the GHZ class and the W class [57]. These two classes, inequivalent under stochastic local operations and classical communication (SLOCC), together span the entire set of three-qubit pure states [57]. We perform an analysis similar to the gW states, and find out how the percentages of states from each class, for which the monogamy score is greater than, equal to, or less than zero, varies with increasing noise parameter $p$ (see [59] for a detailed discussion). The patterns in the W class states are similar to those in the case of gW states, except for discord monogamy score under PD channel. While no gW states have a strictly positive $\delta_{\mathcal{D}}$ for higher values of $p$, in the case of W class states, the corresponding fraction increases with increasing $p$, reaches a maximum value at moderately high $p$, and then, as expected, decreases to zero as $p \to 1$.

### III. CHANNEL DISCRIMINATION VIA MONOGAMY

In this section, we investigate the second objective of this paper, and address the question whether monogamy of quantum correlations can be applied to conclusively detect the type of noise to which the quantum state is exposed. In particular, we propose a two-step protocol to discriminate global noise as well as local channels, namely, AD, PD, and DP channels, via negativity and discord monogamy score, by using a gW state and a gGHZ state as resources. The choice of observable in the second step is determined according to the outcome of the first step. The assumptions required for the success of the protocol are **(i)** that the strength of the noise is moderate, viz., $0.4 \leq p \leq 0.6$, and **(ii)** that the given noisy channel can be used twice. Below,
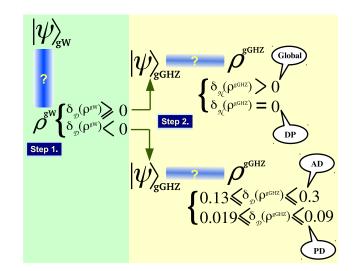


FIG. 4. (Color online.) Schematic representation of the two-step channel discrimination protocol.
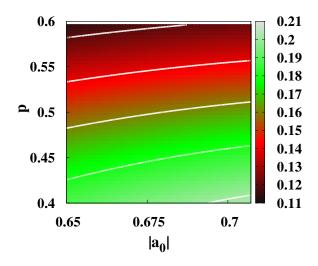


FIG. 5. (Color online.) Variation of $\Delta$, the difference between the values of $\delta_{\mathcal{D}}$ for a fixed gGHZ state under AD and PD channels, with the state parameter, $|a_0|$, and the noise parameter, $p$, in the region "**R**" marked in Fig. 1. The solid lines are obtained by joining constant values of $\Delta$, where from low to high value of $p$, the lines stand for $\Delta = 0.12, 0.14, 0.16, 0.18$, and $0.2$. All quantities plotted are dimensionless, except for $\Delta$, which is in bits.

by an unknown channel, we shall mean one of th four channels, among global noise, AD, PD, and DP channels.

**Two-step discrimination protocol.** The two steps constituting the protocol are as follows. **1.** Given an unknown channel, the first step is to send an arbitrary gW state through that channel and to measure the value of $\delta_{\mathcal{D}}$ for the output state. **2.** The next step is to send a gGHZ state with high entanglement (e.g., $0.65 \leq |a_0| \leq 0.7071$) through the channel, and to measure the monogamy score corresponding to either negativity, or quantum

discord, subject to the outcome of the first step. If $\delta_{\mathcal{D}} \geq 0$ in the first step, $\delta_{\mathcal{N}}$ is chosen as the observable, while for $\delta_{\mathcal{D}} < 0$ in step **1**, discord monogamy score can conclusively identify the type of noise in the channel (as shown schematically in Fig. 4).

Now we explain the implications of the output of the protocol. If $\delta_{\mathcal{D}} < 0$ in step **1** for moderate values of $p$, then the original gW state was subjected to either the AD, or the PD channel, while a nonnegative $\delta_{\mathcal{D}}$ implies that the noise was either global, or DP. This is clear from the variation of the percentages of states for which $\delta_{\mathcal{D}} \geq 0$ and $< 0$ in the range $0.4 \leq p \leq 0.6$, as depicted in Fig. 2. Hence, the first step divides the four types of noise in a block – the duo of AD and PD channels, and global noise and DP channel.

First, let us assume that $\delta_{\mathcal{D}} \geq 0$ in the first step, which leads one to choose $\delta_{\mathcal{N}}$ as observable in the second step of the strategy. For $\delta_{\mathcal{N}} > 0$ in the second step, the type of noise that acts on the gGHZ state is the global noise, while $\delta_{\mathcal{N}} = 0$ implies that the channel is DP. This can be understood from the boxed regions marked "**R**" in Fig. 1, where $\delta_{\mathcal{N}} = 0$ for the DP channel, while $\delta_{\mathcal{N}} > 0$ for global noise. On the other hand, if the outcome of the first step is $\delta_{\mathcal{D}} < 0$, the channel is either AD, or PD. In this situation, $\delta_{\mathcal{D}}$ is always positive when the input state is the gGHZ state with a specific value of $|a_0|$ in the range mentioned before, and so the discrimination protocol is more involved. In particular, we observe that in the marked region "**R**" in Fig. 1, $0.13 \leq \delta_{\mathcal{D}}^{ad} \leq 0.3$ for the AD channel, while for the PD noise, $0.019 \leq \delta_{\mathcal{D}}^{pd} \leq 0.09$. The variation of $\Delta = \delta_{\mathcal{D}}^{ad} - \delta_{\mathcal{D}}^{pd}$, the difference between the values of discord monogamy score in the case of AD channel ($\delta_{\mathcal{D}}^{ad}$) and PD channel ($\delta_{\mathcal{D}}^{pd}$), with $|a_0|$ and $p$ in the region "**R**" in Fig. 1 is plotted in Fig. 5. We notice that there is no overlap between the allowed ranges of $\delta_{\mathcal{D}}$ for the two channels (as also indicated by the absence of the value $\Delta = 0$ in Fig. 5), implying that $\delta_{\mathcal{D}}$ can conclusively distinguish between the AD and the PD channels. The possible encoding of the outcomes of the two-step protocol, and their implications are tabulated in Table II.

**Remark 1.** The first step of our channel discrimination protocol requires not the value, but only the sign of $\delta_{\mathcal{D}}$, while the second step requires an estimation of the discord monogamy score, $\delta_{\mathcal{D}}$, for AD and PD channels.

**Remark 2.** Although the range of values of $\delta_{\mathcal{D}}$ are non-overlapping for AD and PD channels when the state parameter is in the range $0.6 < |a_0| < 0.7071$, the difference between the values corresponding to the lower bound of $\delta_{\mathcal{D}}^{ad}$, and upper bound of $\delta_{\mathcal{D}}^{pd}$ decreases with relaxing the lower bound of $|a_0|$. Hence, the lower bound of the allowed range of $|a_0|$ can be relaxed depending on the accuracy with which $\delta_{\mathcal{D}}^{ad}$ and $\delta_{\mathcal{D}}^{pd}$ can be estimated with the current technology in hand. The best result is

| Step **1**: input gW | Step **2**: input gGHZ | Conclusion |
|---|---|---|
| $\delta_{\mathcal{D}} \geq 0$ | $\delta_{\mathcal{N}} > 0$ | Global noise |
| $\delta_{\mathcal{D}} < 0$ | $0.13 \leq \delta_{\mathcal{D}} \leq 0.3$ | AD Channel |
| $\delta_{\mathcal{D}} < 0$ | $0.019 \leq \delta_{\mathcal{D}} \leq 0.09$ | PD Channel |
| $\delta_{\mathcal{D}} \geq 0$ | $\delta_{\mathcal{N}} = 0$ | DP channel |

TABLE II. Encoding of the outcomes of the two-step channel discrimination protocol using monogamy scores of negativity and quantum discord.

obtained for the three-qubit GHZ state, for which $|a_0| = 1/\sqrt{2}$.
**Remark 3.** In the presence of high noise ($p > 0.6$), our protocol may fail to distinguish the type of noise applied to the quantum state. This is because both $\delta_{\mathcal{D}}$ and $\delta_{\mathcal{N}}$ may vanish in the case of both gGHZ state and gW state when the noise strength is high. It is also clear that the above distinguishing protocol fails when $p \approx 0$.

## IV. CONCLUSION

The question that naturally arises from the results reported in the preceeding sections is whether the dynamical features found in the case of three-qubit systems is generic for quantum states with higher number of qubits. The study of the dynamical properties of monogamy scores in the multipartite domain with more than three parties is challenging due to computational as well as analytical difficulties in computing the correlation measures. In particular, the number of inequivalent SLOCC classes with higher number of parties becomes much higher [57]. As we have already mentioned, the monogamy score of gGHZ state decreases monotonically with the increase of $p$ for an arbitrary number of parties. And, the non-monotonic behaviour of the monogamy scores corresponding to both negativity and quantum discord, in the case of the three-qubit generalized W state under, for example, the AD channel, is found in the case of higher number of qubits (see [59]). We also find that similar to the three-qubit scenario, the depolarizing channel destroys the monogamy scores corresponding to both negativity and quantum discord more rapidly compared to other channels, for four qubits. We therefore expect that the broad qualitative features of the results found in the case of three qubits remain unaltered when the number of qubits is increased.

Summarizing, we have investigated the patterns of the monogamy property of quantum correlations using monogamy score as the observable, when three-qubit systems are subjected to global noise as well as local noisy channels, viz. amplitude-damping, phase-damping, and depolarizing channels. As the quantum correlation measures that are used to constitute the monogamy score, we chose negativity and quantum discord, and found that the dynamics of monogamy score, when generalized GHZ states are subjected to different types of noise, is qualitatively different from that of the generalized W state as input. While monogamy score corresponding to both the quantum correlation measures exhibit a monotonic decay with increasing noise in the former case, non-monotonic dynamics takes place in the latter, giving rise to a rich set of dynamical profiles. We define a characteristic noise scale, called the "dynamics terminal", that quantifies the persistence of the monogamy score corresponding to a particular measure of quantum correlation, when the state is subjected to a specific type of noise. We show that the dynamics terminal can distinguish between the different noise models, and indicates that the depolarizing channel destroys monogamy scores faster compared to the other types of noise. To investigate how the monogamy property behaves against increasing noise, we investigate the variation of the fraction of states with increasing value of the noise parameter, when the input states are chosen from the GHZ and the W class. We also show that the negativity monogamy score may

exhibit a more robust behavior against phase damping noise, compared to the discord monogamy score, which is in contrast to the usual observation regarding bipartite entanglement measures and quantum discord. As an usefulness of such study, we propose a two-step channel discrimination protocol that can conclusively identify the different types of noise by considering monogamy scores and by using the gGHZ and the gW states as resources.

[1] R. Horodecki, P. Horodecki, M. Horodecki, and K. Horodecki, Rev. Mod. Phys. **81**, 865 (2009), and the references therein.

[2] L. C. Céleri, J. Maziero, and R. M. Serra, Int. J. Quant. Inf. **9**, 1837 (2011), and the references therein.

[3] K. Modi, A. Brodutch, H. Cable, T. Paterek, and V. Vedral, Rev. Mod. Phys. **84**, 1655 (2012), and the references therein.

[4] L. Henderson and V. Vedral, J. Phys. A: Math. Gen. **34**, 6899 (2001); H. Ollivier and W. H. Zurek, Phys. Rev. Lett. **88**, 017901 (2001).

[5] J. Oppenheim, M. Horodecki, P. Horodecki and R. Horodecki, Phys. Rev. Lett. **89**, 180402 (2002); M. Horodecki, K. Horodecki, P. Horodecki, R. Horodecki, J. Oppenheim, A. Sen(De), and U. Sen, Phys. Rev. Lett. **90**, 100402 (2003); I. Devetak, Phys. Rev. A **71**, 062303 (2005); M. Horodecki, P. Horodecki, R. Horodecki, J. Oppenheim, A. Sen(De), U. Sen, and B. Synak-Radtke, Phys. Rev. A **71**, 062307 (2005).

[6] B. Dakić, V. Vedral, and Č. Brukner, Phys. Rev. Lett. **105**, 190502 (2010); S. Luo and S. Fu, Phys. Rev. A **82**, 034302 (2010); X. -M. Lu, Z. -J. Xi, Z. Sun, and X. Wang, Quant. Info. Comput., **10**, 0994 (2010); D. Girolami and G. Adesso, Phys. Rev. A **84**, 052110 (2011); T. Debarba, T. O. Maciel, and R. O. Vianna, Phys. Rev. A **86**, 024302 (2012); J. -S. Jin, F. -Y Zhang, C.-S. Yu, and H. -S. Song, J. Phys. A: Math. Theor. **45**, 115308 (2012); J. D. Montealegre, F. M. Paula, A. Saguia, and M. S. Sarandy, Phys. Rev. A **87**, 042115 (2013); D. Spehner and M. Orszag, New J. Phys. **15**, 103001 (2013); D. Girolami and G. Adesso, Phys. Rev. A **84**, 052110 (2011); M. Piani, Phys. Rev. A **86**, 034101 (2012); F. M. Paula, Thiago R. de Oliveira, and M. S. Sarandy, Phys. Rev. A **87**, 064101 (2013); F. Ciccarello, T. Tufarelli, and V Giovannetti, New J. Phys. **16**, 013038 (2014); D. Spehner and M. Orszag, J. Phys. A: Math. Theor. **47**, 035302 (2014).

[7] C. H. Bennet and S. J. Wiesner, Phys. Rev. Lett. **69**, 2881 (1992); K. Mattle, H. Weinfurter, P. G. Kwiat, and A. Zeilinger, Phys. Rev. Lett. **76**, 4656 (1996).

[8] M. Żukowski, A. Zeilinger, M. Horne, and H. Weinfurter, Acta Phys. Pol. **93**, 187 (1998); Mark Hillery, Vladimir Buzek, and Andr Berthiaume, Phys. Rev. A **59**, 1829 (1999); R. Demkowicz-Dobrzanski, Aditi Sen(De), Ujjwal Sen, and Maciej Lewenstein, Phys. Rev. A **80**, 012311 (2009); N. Gisin, Grégoire Ribordy, Wolfgang Tittel, and Hugo Zbinden, Rev. Mod. Phy. **74**, 145 (2002); R. Cleve, Daniel Gottesman, and Hoi-Kwong Lo, Phys. Rev. Lett. **83**, 648 (1999); A. Karlsson, Masato Koashi, and Nobuyuki Imoto, Phys. Rev. A **59**, 162 (1999).

[9] C. H. Bennett, G. Brassard, C. Crépeau, R. Jozsa, A. Peres, and W. K. Wootters, Phys. Rev. Lett. **70**, 1895 (1993); D. Bouwmeester, J. W. Pan, K. Mattle, M. Eibl, H. Weinfurter, and A. Zeilinger, Nature **390**, 575 (1997); J. W. Pan, D. Bouwmeester, H. Weinfurter, and A. Zeilinger, Phys. Rev. Lett. **80**, 3891 (1998); D. Bouwmeester, J. W. Pan, H. Weinfurter, and A. Zeilinger, J. Mod. opt. **47**, 279 (2000).

[10] A. Acín, N. Brunner, N. Gisin, S. Massar, S. Pironio, and V. Scarani, Phys. Rev. Lett. **98**, 230501 (2007); S. Pironio, A. Acín, N. Brunner, N. Gisin, S. Massar, and V. Scarani, New J. Phys. **11**, 045021 (2009); N. Gisin, S. Pironio, and N. Sangouard, Phys. Rev. Lett. **105**, 070501 (2010); L. Masanes, S. Pironio, and A. Acín, Nature Commun. **2**, 238 (2011); H. K. Lo, M. Curty, and B. Qi, Phys. Rev. Lett. **108**, 130503 (2012).

[11] A. Ekert, Phys. Rev. Lett. **67**, 661 (1991); T. Jennewein, C. Simon, G. Weihs, H. Weinfurter, and A. Zeilinger, Phys. Rev. Lett. **84**, 4729 (2000); D. S. Naik, C. G. Peterson, A. G. White, A. J. Berglund, and P. G. Kwiat, Phys. Rev. Lett. **84**, 4733 (2000); W. Tittel, T. Brendel, H. Zbinden, and N. Gisin, Phys. Rev. Lett. **84**, 4737 (2000); N. Gisin, G. Ribordy, W. Tittel, and H. Zbinden, Rev. Mod. Phys. **74**, 145 (2002).

[12] A. Sen(De) and U. Sen, Physics News **40**, 17 (2010) (arXiv:1105.2412 [quant-ph]).

[13] R. Raussendorf and H. J. Briegel, Phys. Rev. Lett. **86**, 5188 (2001); P. Walther, K. J. Resch, T. Rudolph, E. Schenck, H. Weinfurter, V. Vedral, M. Aspelmeyer, and A. Zeilinger, Nature **434**, 169 (2005); H. J. Briegel, D. Browne, W. Dür, R. Raussendorf, and M. van den Nest, Nat. Phys. **5**, 19 (2009).

[14] C. H. Bennett, D. P. DiVincenzo, C. A. Fuchs, T. Mor, E. Rains, P. W. Shor, J. A. Smolin, and W. K. Wootters, Phys. Rev. A **59**, 1070 (1999); C. H. Bennett, D.P. DiVincenzo, T. Mor, P.W. Shor, J.A. Smolin, and B.M. Terhal, Phys. Rev. Lett. **82**, 5385 (1999); D. P. DiVincenzo, T. Mor, P. W. Shor, J. A. Smolin, and B. M. Terhal Commun. Math. Phys. **238**, 379 (2003).

[15] A. Peres and W.K. Wootters, Phys. Rev. Lett. **66**, 1119 (1991); J. Walgate, A.J. Short, L. Hardy, and V. Vedral,ibid. **85**, 4972 (2000); S. Virmani, M.F. Sacchi, M.B. Plenio, and D. Markham, Phys. Lett. A **288**, 62 (2001); Y.-X. Chen and D. Yang, Phys. Rev. A **64**, 064303 (2001);ibid. **65**, 022320 (2002); J. Walgate and L. Hardy, Phys. Rev. Lett. **89**, 147901 (2002); M. Horodecki, A. Sen(De), U. Sen, and K. Horodecki, ibid. **90**, 047902 (2003); W. K. Wootters, Int. J. Quantum Inf. **4**, 219 (2006).

[16] E. Knill and R. Laflamme, Phys. Rev. Lett. **81**, 5672 (1998); A. Datta, A. Shaji, and C. M. Caves, Phys. Rev. Lett. **100**, 050502 (2008); B. P. Lanyon, M. Barbieri, M. P. Almeida, and A. G. White, Phys. Rev. Lett. **101**, 200501 (2008).

[17] L. Roa, J. C. Retamal, and M. Alid-Vaccarezza, Phys. Rev. Lett. **107**, 080401 (2011); V. Madhok and A. Datta, Phys. Rev. A **83**, 032323 (2011); V. Madhok and A. Datta, Int. J. Mod. Phys. B **27**, 1345041 (2013).

[18] B. Dakić, Y. O. Lipp, X. Ma, M. Ringbauer, S. Kropatschek, S. Barz, T. Paterek, V. Vedral, A. Zeilinger, Časlav Brukner, and P. Walther, Nature Phys. **8**, 666 (2012).

[19] J. M. Raimond, M. Brune, S. Haroche, Rev. Mod. Phys. **73**, 565 (2001); D. Leibfried, R. Blatt, C. Monroe, and D. Wineland, Rev. Mod. Phys. **75**, 281 (2003); L. M. K. Vandersypen, I.L Chuang, Rev. Mod. Phys. **76**, 1037 (2005); K. Singer, U. Poschinger, M. Murphy, P. Ivanov, F. Ziesel, T. Calarco, F. Schmidt-Kaler, Rev. Mod. Phys. **82**, 2609 (2010); H. Haffner, C. F. Roose, R. Blatt, Phys. Rep. **469**, 155 (2008); L.-M. Duan, C. Monroe, Rev. Mod. Phys. **82**, 1209 (2010); J.-W. Pan, Z.-B. Chen, C.-Y. Lu, H. We-

infurter, A. Zeilinger, M. Żukowski, Rev. Mod. Phys. **84**, 777 (2012).

[20] M. A. Yurishchev, Phys. Rev. B **84**, 024418 (2011); R. Auccaise, J. Maziero, L. C. Céleri, D. O. Soares-Pinto, E. R. deAzevedo, T. J. Bonagamba, R. S. Sarthour, I. S. Oliveira, and R. M. Serra, Phys. Rev. Lett. **107**, 070501 (2011); G. Passante, O. Moussa, D. A. Trottier, and R. Laflamme, Phys. Rev. A **84**, 044302 (2011); L. S. Madsen, A. Berni, M. Lassen, and U. L. Andersen, Phys. Rev. Lett. **109**, 030402 (2012). M. Gu, H. M. Chrzanowski, S. M. Assad, T. Symul, K. Modi, T. C. Ralph, V. Vedral, and P. K. Lam, Nature Phys. **8**, 671 (2012); R. Blandino, M. G. Genoni, J. Etesse, M. Barbieri, M. G. A. Paris, P. Grangier, and R. Tualle-Brouri, Phys. Rev. Lett. **109**, 180402 (2012); U. Vogl, R. T. Glasser, Q. Glorieux, J. B. Clark, N. V. Corzo, and P. D. Lett, Phys. Rev. A **87**, 010101(R) (2013); C. Benedetti, A. P. Shurupov, M. G. A. Paris, G. Brida, and M. Genovese, Phys. Rev. A **87**, 052136 (2013).

[21] Á. Rivas and S. F. Huelga, Open Quantum Systems : An Introduction (Springer Briefs in Physics, 2012); Á. Rivas, S. F. Huelga, and M. B. Plenio, Rep. Prog. Phys. **77**, 094001 (2014).

[22] K. Zyczkowski, P. Horodecki, M. Horodecki, and R. Horodecki, Phys. Rev. A **65**, 012101 (2001); L. Diósi, Lec. Notes Phys. **622**, 157 (2003); P. J. Dodd and J. J. Halliwell, Phys. Rev. A **69**, 052105 (2004); T. Yu and J. H. Eberly, Phys. Rev. Lett. **93**, 140404 (2004). M. O. Terra Cunha, New J. Phys. **9**, 237 (2007).

[23] M. P. Almeida, F. de Melo, M. Hor-Meyll, A. Salles, S. P. Walborn, P. H. S. Ribeiro, and L. Davidovich, Science **316**, 579 (2007); A. Salles, F. de Melo, M. P. Almeida, M. Hor-Meyll, S. P. Walborn, P. H. S. Ribeiro, and L. Davidovich, Phys. Rev. A **78**, 022322 (2008); T. Yu and J. H. Eberly, Science **323**, 598 (2009).

[24] J. Maziero, T. Werlang, F. F. fanchini, L. C. Céleri, and R. M. Serra, Phys. Rev. A **81**, 022116 (2010).

[25] T. Werlang, S. Souza, F. F. Fanchini, and C. J. V. Boas, Phys. Rev. A **80**, 024103 (2009); J. Maziero, L. C. Céleri, R. M. Serra, and V. Vedral, Phys. Rev. A **80**, 044102 (2009); K. Berrada, H. Eleuch, and Y. Hassouni, J. Phys. B: At. Mol. Opt. Phys. **44**, 145503 (2011); A. K. Pal, and I. Bose, Eur. Phys. J. B **85**, 277 (2012); J. P. G. Pinto, G. Karpat, and F. F. Fanchini, Phys. Rev. A **88**, 034304 (2013).

[26] B. Wang, Z-Y Xu, Z-Q Chen, and M. Feng, Phys. Rev. A **81**, 014101 (2010); F. F. Fanchini, T. Werlang, C. A. Brasil, L. G. E. Arruda, and A. O. Caldeira, Phys. Rev. A **81**, 052107 (2010); F. Altintas and R. Eryigit, Phys. Lett. A **374**, 4283 (2010); Z. Y. Xu, W. L. Yang, X. Xiao, and M. Feng, J. Phys. A: Math. Theor. **44**, 395304 (2011); B. Bellomo, G. Compagno, R. Lo Franco, A. Ridolfo, S. Savasta, Int. J. Quant. Inf. **9**, 1665 (2011); Z. Xi, X.-M. Lu, Z. Sun, and Y. Li, J. Phys. B: At. Mol. Opt. Phys. **44**, 215501 (2011); R. Lo Franco, B. Bellomo, S. Maniscalco, and G. Compagno, Int. J. Mod. Phys. B **27**, 1345053 (2013).

[27] M. Daoud and R. A. Laamara, J. Phys. A: Math. Theor. **45**, 325302 (2012); J. -S. Xu, K. Sun, C. -F. Li, X. -Y. Xu, G.-C. Guo, E. Andersson, R. Lo Franco, and G. Compagno, Nat. Comm. **4**, 2851 (2013).

[28] L. Mazzola, J. Piilo and S. Maniscalco, Phys. Rev. Lett. **104**, 200401 (2010); B. Aaronson, R. L. Franco, and G. Adesso, Phys. Rev. A **88**, 012120 (2013); L. Mazzola, J. Piilo, and S. Maniscalco, Int. J. Quantum Inform. **9**, 981 (2011); Q -L He, J-B Xu, D-X Yao, and Y-Q Zhang, Phys. Rev. A **84**, 022312 (2011); G. Karpat and Z. Gedik, Phys. Lett. A **375**, 4166 (2011); Y.-Q. Lü, J.-H. An, X.-M. Chen, H.-G. Luo, and C. H. Oh, Phys. Rev. A **88**, 012129 (2013); G. Karpat and Z. Gedik, Phys. Scr. **T153**, 014036 (2013); J.-L. Guo, H. Li, and G.-L. Long, Quant. Info. Process. **12**, 3421 (2013); P. Haikka, T. H. Johnson, and S. Maniscalco, Phys. Rev. A **87**, 010103(R) (2013); J. D. Montealegre, F. M. Paula, A. Saguia, and M. S. Sarandy, Phys. Rev. A **87**, 042115 (2013);

[29] T. Chanda, A. K. Pal, A. Biswas, A. Sen(De), and U. Sen, Phys. Rev. A **91**, 062119 (2015).

[30] E. G. Carnio, A. Buchleitner, and M. Gessner, Phys. Rev. Lett. **115**, 010404 (2015).

[31] A. R. R. Carvalho, F. Mintert, and A. Buchleitner, Phys. Rev. Lett. **93**, 230501 (2004); W. Dür and H.-J. Briegel, Phys. Rev. Lett. **92**, 180403 (2004); M. Hein, W. Dür, and H.-J. Briegel, Phys. Rev. A **71**, 032350 (2005); A. Montakhab and A. Asadian, Phys. Rev. A **77**, 062322 (2008); L. Aolita, D. Cavalcanti, A. Acín, A. Salles, M. Tiersch, A. Buchleitner, and F. de Melo, Phys. Rev. A **79**, 032322 (2009); Z. Ma, Z. Chen, and F. F. Fanchini, New J. Phys. **15**, 043023 (2013).

[32] V. Coffman, J. Kundu, and W. K. Wootters, Phys. Rev. A **61**, 052306 (2000).

[33] B. Terhal, IBM J. Res. Dev. **48**, 71 (2004).

[34] C. H. Bennett, H. J. Bernstein, S. Popescu, and B. Schumacher, Phys. Rev. A **53**, 2046 (1996); M. Christandl and A. Winter, J. Math. Phys. (N.Y.) **45**, 829 (2004). T. J. Osborne and F. Verstraete, Phys. Rev. Lett. **96**, 220503 (2006); Y.-C. Ou and H. Fan, Phys. Rev. A **75**, 062308 (2007); B. Toner and F. Verstraete, arXiv:quant-ph/0611001; M. Hayashi and L. Chen, Phys. Rev. A **84**, 012325 (2011); R. Ramanathan, A. Soeda, P. Kurzynski, and D. Kaszlikowski, Phys. Rev. Lett. **109**, 050404 (2012); P. Kurzynski, A. Cabello, and D. Kaszlikowski, Phys. Rev. Lett. **112**, 100401 (2014); Y-K. Bai, Y-F. Xu, and Z. D. Wang, Phys. Rev. Lett. **113**, 100503 (2014); T. R. de Oliveira, M. F. Cornelio, and F. F. Fanchini, Phys. Rev. A **89**, 034303 (2014).

[35] M. Koashi and A. Winter, Phys. Rev. A **69**, 022309 (2004).

[36] T. J. Osborne and F. Verstraete, Phys. Rev. Lett. **96**, 220503 (2006); G. Adesso, A. Serafini, and F. Illuminati, Phys. Rev. A **73**, 032345 (2006); T. Hiroshima, G. Adesso, and F. Illuminati, Phys. Rev. Lett. **98**, 050503 (2007); M. Seevinck, Phys. Rev. A **76**, 012106 (2007); M. Seevinck, Quant. Info. Proc. **9**, 273 (2010); M.-J. Zhao, S.-M. Fei, and Z.-X. Wang, Int. J. Quant. Inform. **8**, 905 (2010); G. L. Giorgi, Phys. Rev. A **84**, 054301 (2011); F. F. Fanchini, M. F. Cornelia, M. C. de Oliveira, and A. O. Caldeira, Phys. Rev. A **84**, 012313 (2011); A. Sen(De) and U. Sen, Phys. Rev. A **85**, 052103 (2012); R. Prabhu, A. K. Pati, A. Sen(De), and U. Sen, Phys. Rev. A **85**, 040102(R) (2012); A. Streltsov, G. Adesso, M. Piani, D. Bruß, Phys. Rev. Lett. **109**, 050503 (2012); H. C. Braga, C. C. Rulli, T. R. de Oliveira, and M. S. Sarandy, Phys. Rev. A **86**, 062106 (2012); X.-J. Ren and H. Fan, Quantum Inf. Comput. **13**, 0469 (2013); X.-K. Song, T. Wu, and L. Ye, Mod. Phys. Lett. B **27**, 1350049 (2013); K. Salini, R. Prabhu, A. Sen(De), and U. Sen, Ann. Phys. **348**, 297 (2014); A. Kumar, R. Prabhu, A. Sen(De), and U. Sen, Phys. Rev. A **91**, 012341 (2015).

[37] R. Prabhu, A. K. Pati, A. Sen(De), and U. Sen, Phys. Rev. A **86**, 052337 (2012).

[38] B. Toner, Proc. R. Soc. A **465**, 59 (2009); M. P. Seevinck, Quant. Inf. Proc. **9**, 273 (2010).

[39] A. K. Ekert, Phys. Rev. Lett. **67**, 661 (1991); J. Barrett, L. Hardy, and A. Kent, Phys. Rev. Lett. **95**, 010503 (2005); M. Tomamichel, S. Fehr, J. Kaniewski, and S. Wehner, New J. Phys. **15**, 103002 (2013); U. Vazirani and T. Vidick, Phys. Rev. Lett. **113**, 140501 (2014).

[40] S. Lee and J. Park, Phys. Rev. A **79**, 054309 (2009); A. Kay, D. Kaszlikowski, and R. Ramanathan, Phys. Rev. Lett. **103**, 050501 (2009).

[41] R. Prabhu, A. K. Pati, A. Sen(De), and U. Sen, Phys. Rev. A **87**, 052319 (2013).

[42] M. D. Reid, Phys. Rev. A **88**, 062108 (2013); A. Milne, S. Jevtic, D. Jennings, H. Wiseman, and T. Rudolph, New J. Phys. **16**,

083017 (2014).

[43] X.-S. Ma, B. Dakic, W. Naylor, A. Zeilinger, and P. Walther, Nat. Phys. **7**, 399 (2011); F. G. S. L. Brandao and A. W. Harrow; Proceedings of the 45th ACM Symposium on theory of computing, pp. 861 (2013); A. García-Sáez and J. I. Latorre, Phys. Rev. B **87**, 085130 (2013).

[44] L. Susskind, arXiv:1301.4505 (2013); S. Lloyd and J. Preskill, J. High. En. Phys. **08**, 126 (2014).

[45] K. R. K. Rao, H. Katiyar, T. S. Mahesh, A. Sen(De), U. Sen, and A. Kumar, Phys. Rev. A **88**, 022312 (2013).

[46] J. Lee, M. S. Kim, Y. J. Park, and S. Lee, J. Mod. Opt. **47**, 2151 (2000); G. Vidal and R.F. Werner, Phys. Rev. A **65**, 032314 (2002); M. B. Plenio, Phys. Rev. Lett. **95**, 090503 (2005).

[47] A. Peres, Phys. Rev. Lett. **77**, 1413 (1996); M. Horodecki, P. Horodecki, and R. Horodecki, Phys. Lett. A **223**, 1 (1996).

[48] W. H. Zurek, in Quantum Optics, Experimental Gravitation and Measurement Theory, edited by P. Meystre and M. O. Scully (Plenum, New York, 1983); S. M. Barnett and S. J. D. Phoenix, Phys. Rev. A **40**, 2404 (1989). B. Schumacher and M. A. Nielsen, Phys. Rev. A **54**, 2629 (1996); N. J. Cerf and C. Adami, Phys. Rev. Lett. **79**, 5194 (1997); B. Groisman, S. Popescu, and A. Winter, Phys. Rev. A **72**, 032317 (2005).

[49] E. C. G. Sudarshan, P. M. Mathews, and J. Rau, Phys. Rev. **121**, 920 (1961).

[50] K. Kraus, Ann. Phys., **64**, 311, (1971).

[51] M. Choi, Linear Algebra and Its Applications **10**, 285 (1975).

[52] K. Kraus, *States, Effects and Operations: Fundamental Notions of Quantum Theory*, Lecture Notes in Physics, Vol. **190**, Springer-Verlag, Berlin, 1983.

[53] J. Preskill, *Quantum Information and Computation*, Lect. Notes available at http://www.theory.caltech.edu/ people/preskill/ph229/#lecture.

[54] D. M. Greenberger, M. A. Horne, and A. Zeilinger, in Bell's Theorem, Quantum Theory, and Conceptions of the Universe, ed. M. Kafatos (Kluwer Academic, Dordrecht, The Netherlands, 1989).

[55] A. Zeilinger, M. A. Horne, and D. M. Greenberger, in Proceedings of Squeezed States and Quantum Uncertainty, edited by D. Han, Y. S. Kim, and W. W. Zachary, NASA Conf. Publ. **3135**, 73 (1992).

[56] A. Sen(De), U. Sen, M. Wiesniak, D. Kaszlikowski, and M. Żukowski, Phys. Rev. A **68**, 062306 (2003).

[57] W. Dür, G. Vidal, J. I. Cirac, Phys. Rev. A **62**, 062314 (2000).

[58] A. Fujiwara, Phys. Rev. A **63**, 042304 (2001); M. Sarovar and G. J. Milburn, J. Phys. A: Math. Gen. **39**, 8487 (2006).

[59] See supplementary materials.

[60] Y. Huang, New. J. Phys. **16** (3), 033027 (2014).

[61] S. Luo, Phys. Rev. A **77**, 042303 (2008).

[62] M. Ali, A. R. P. Rau, and G. Alber, Phys. Rev. A **81**, 042105 (2010); *ibid.* **82**, 069902(E) (2010); X.-M. Lu, J. Ma, Z. Xi, and X. Wang, Phys. Rev. A **83**, 012327 (2011); D. Girolami and G. Adesso, Phys. Rev. A **83**, 052108 (2011); Q. Chen, C. Zhang, S. Yu, X. X. Yi, and C. H. Oh, Phys. Rev. A **84**, 042313 (2011).

[63] Y. Huang, Phys. Rev. A **88**, 014302 (2013); M. Namkung, J. Chang, J. Shin, and Y. Kwon, arXiv: 1404.6329 [quant-ph] (2014).

[64] F. F. Fanchini, T. Werlang, C. A. Brasil, L. G. E. Arruda, and A. O. Caldeira, Phys. Rev. A **81**, 052107 (2010); B. Li, Z. -X. Wang, and S. -M. Fei, Phys. Rev. A **83**, 022321 (2011).

[65] T. Chanda, T. Das, D. Sadhukhan, A. K. Pal, A. Sen(De), and U. Sen, Phys. Rev. A **92**, 062301 (2015).

# Supplementary Materials
## Conclusive Identification of Quantum Channels via Monogamy of Quantum Correlations

Asutosh Kumar[1,2], Sudipto Singha Roy[1,2], Amit Kumar Pal[1,2], R. Prabhu[1,2,3], Aditi Sen(De)[1,2], and Ujjwal Sen[1,2]

[1]Harish-Chandra Research Institute, Chhatnag Road, Jhunsi, Allahabad 211019, India
[2]Homi Bhabha National Institute, Training School Complex, Anushaktinagar, Mumbai 400094, India
[3]Department of Physics, Indian Institute of Technology Patna, Bihta 801103, Bihar, India

## SSEC1.   MEASURES OF QUANTUM CORRELATIONS

In this paper, we restrict ourselves to two specific measures, namely, negativity and quantum discord. The first one belongs to the quantum correlations defined in the entanglement-separability domain, while the second one is an information-theoretic quantum correlation measure.

*Negativity.* For a bipartite state $\rho_{AB}$, its negativity [SR1], $\mathcal{N}(\rho_{AB})$, is defined as the absolute value of the sum of the negative eigenvalues of $\rho_{AB}^{T_A}$, where $\rho_{AB}^{T_A}$ denotes the partial transpose [SR2] of $\rho_{AB}$ with respect to the subsystem $A$. Alternatively, it is expressed as

$$\mathcal{N}(\rho_{AB}) = \frac{\|\rho_{AB}^{T_A}\|_1 - 1}{2}, \tag{SEQ1}$$

where $\|M\|_1 \equiv \mathrm{tr}\sqrt{M^\dagger M}$ is the trace-norm of the matrix $M$.

*Quantum Discord.* Quantum discord [SR3] is defined as the difference between the "total correlation" [SR4] and the "classical correlation" [SR3] present in the composite system, described by the bipartite state $\rho_{AB}$. The total correlation can be quantified as the quantum mutual information, and is given by

$$\mathcal{I}(\rho_{AB}) = S(\rho_A) + S(\rho_B) - S(\rho_{AB}), \tag{SEQ2}$$

where $S(\varrho) = -\mathrm{tr}(\varrho \log_2 \varrho)$ is the von Neumann entropy of $\varrho$, and $\rho_{A(B)}$ are the local density matrices of $\rho_{AB}$, obtained as $\rho_{A(B)} = \mathrm{tr}_{B(A)}[\rho_{AB}]$. On the other hand, the classical correlation is defined as

$$\mathcal{J}(\rho_{AB}) = S(\rho_B) - S(\rho_{B|A}), \tag{SEQ3}$$

where the conditional entropy, $S(\rho_{B|A})$, is given by

$$S(\rho_{B|A}) = \min_{\{P_i\}} \sum_i p_i S(\rho_{B|i}). \tag{SEQ4}$$

Here, $S(\rho_{B|A})$ is conditioned over measurement performed on $A$ with a rank-one projection-valued measurements $\{P_i\}$, producing the states $\rho_{B|i} = \frac{1}{p_i}\mathrm{tr}_A[(P_i \otimes \mathbb{I}_B)\rho_{AB}(P_i \otimes \mathbb{I}_B)]$, with probability $p_i = \mathrm{tr}[(P_i \otimes \mathbb{I}_B)\rho_{AB}(P_i \otimes \mathbb{I}_B)]$, $\mathbb{I}_B$ being the identity operator in the Hilbert space of $B$. From Eqs. (SEQ2) and (SEQ3), quantum discord can be obtained as

$$\mathcal{D}(\rho_{AB}) = \mathcal{I}(\rho_{AB}) - \mathcal{J}(\rho_{AB}). \tag{SEQ5}$$

**Note.** The difficulty in the computation of quantum discord arises due to the optimization involved in the definition of classical correlation of the state $\rho_{AB}$ [SR5]. In the case of a pure bipartite state $\rho_{AB}$, quantum discord reduces to $S(\rho_A)$, the von Neumann entropy of the local density matrix $\rho_A$ [SR6]. On the other hand, there are only a few examples of mixed bipartite states, for which quantum discord can be obtained analytically [SR7, SR8]. For an arbitrary mixed bipartite state $\rho_{AB}$, computation of quantum discord involves adaptation of numerical optimization techniques [SR9]. In the case of a $\mathbb{C}^2 \otimes \mathbb{C}^d$ system, if measurement is performed on the qubit, the rank-1 projectors, $\{P_i = |\Phi_i\rangle\langle\Phi_i|, i = 1, 2\}$, can be parametrized as

$$|\Phi_1\rangle = \cos\frac{\theta}{2}|0\rangle + e^{i\phi}\sin\frac{\theta}{2}|1\rangle,$$
$$|\Phi_2\rangle = -e^{-i\phi}\sin\frac{\theta}{2}|0\rangle + \cos\frac{\theta}{2}|1\rangle. \tag{SEQ6}$$

The optimization, in this case, is to be performed over the space of the real parameters $(\theta, \phi)$, where $0 \leq \theta \leq \pi$ and $0 \leq \phi < 2\pi$.

## SSEC2.   MONOGAMY OF QUANTUM CORRELATIONS

Let us now introduce the concept of monogamy [SR10] for a quantum correlation measure, $\mathcal{Q}$. Monogamy helps in exploring the amount of quantum correlations shared among the subsystems of a quantum system. All the known quantum correlation measures

qualitatively follow a monogamy relation. In the case of a tripartite system, it implies that if two of the parties are maximally quantum correlated, then there can not be any quantum correlation between either of these two parties with the third one. Importantly, classical correlations do not have such restrictions. We will now quantify the monogamy constraint for an arbitrary bipartite quantum correlation measure, say $\mathcal{Q}$. An $n$-party state, $\rho_{A_1 A_2 \cdots A_n}$, shared between the parties, $A_1, A_2, \cdots, A_n$, is said to be monogamous under the quantum correlation measure $\mathcal{Q}$, if it follows the monogamy inequality given by

$$\mathcal{Q}(\rho_{A_1:A_2\cdots A_n}) \geq \sum_{j=2}^{n} \mathcal{Q}(\rho_{A_1 A_j}), \tag{SEQ7}$$

where $\rho_{A_1 A_j}$ is obtained from $\rho_{A_1 A_2 \cdots A_n}$ by tracing out all the parties except $A_1$ and $A_j$. Otherwise, it is non-monogamous. Here we call the party $A_1$ as the nodal observer. In this respect, the "monogamy score" with respect to $\mathcal{Q}$, for the $n$-party state, $\rho_{A_1 A_2 \cdots A_n}$, is defined as [SR11]

$$\delta_{\mathcal{Q}} = \mathcal{Q}(\rho_{A_1:A_2\cdots A_n}) - \sum_{j=2}^{n} \mathcal{Q}(\rho_{A_1 A_j}). \tag{SEQ8}$$

Therefore, positivity of $\delta_{\mathcal{Q}}$ for a given quantum state implies monogamy of quantum correlation measure $\mathcal{Q}$ for that state.
**Note.** The choice of measurement, in the definition of quantum discord, puts an inherent asymmetry in the measure. In this paper, unless otherwise stated, the measurement is performed on the first subsystem of the bipartite quantum system. This implies that while computing $\mathcal{D}(\rho_{A_1 A_j})$ to determine $\delta_{\mathcal{Q}}$, the measurement is always performed on the nodal observer.


### SSEC3. DECOHERENCE UNDER GLOBAL AND LOCAL NOISE

A quantum system inevitably interacts with its environment and eventually decoheres, and looses its quantum correlations. Such a decohering process can be described by a completely positive trace preserving (CPTP) map, $\mathcal{E}$, which, acting on the quantum system, $\rho$, transforms the state as [SR12–SR18]

$$\rho \rightarrow \rho' = \mathcal{E}(\rho). \tag{SEQ9}$$

The noise can act either globally, or locally on each subsystem of the system of interest. In the present study, we consider both the scenarios.
**Global noise.** In this case, we consider an environment that acts globally on a system of dimension $d^n$ and in the state $\rho$, for which the resulting state is given by

$$\rho' = \frac{p}{d^n} I + (1-p)\rho, \tag{SEQ10}$$

where $p$ is the mixing parameter ($0 \leq p \leq 1$), and $I$ is the identity operator in the Hilbert space of the system. Note that $p = 0$ stands for the noiseless case, while $p = 1$ corresponds to the fully decohered state.
**Local noise.** For a composite quantum system having $n$ spatially separated subsystems, it is reasonable to assume that the environment acts independently and locally on each of the subsystems. We now briefly describe various such local noisy channels.
The dynamics of a closed quantum system is described by a unitary transformation. To describe the dynamics of an open quantum system, which is interacting with its environment, one can assume that the system and the environment together form a closed quantum system, whose state, $\rho$, is given by $\rho = \rho_s \otimes \rho_e$, with $\rho_s$ and $\rho_e$ being respectively the states of the system and the environment. The next step would be to apply a unitary transformation to the given composite system and finally trace out the environment part to obtain the reduced state of the changed system. In this case, quantum operations can be considered in the *operator-sum representation* [SR15], written explicitly in terms of operators on the Hilbert space of the system as follows:

$$\rho'_s = \text{tr}_e[U(\rho_s \otimes \rho_e)U^{\dagger}] = \sum_k E_k \rho_s E_k^{\dagger}, \tag{SEQ11}$$

where the operators $\{E_k\}$ are known as Kraus operators [SR12, SR15, SR17, SR18] and satisfy $\sum_k E_k^{\dagger} E_k = I$. For a system "$s$" of dimension $d$, any quantum operation can be represented by at most $d^2$ Kraus operators.
For an $n$-partite system, $\rho_{A_1 A_2 \cdots A_n}$, in arbitrary dimensions, after the actions of the local environments on the subsystems, the evolved state, $\rho'_{A_1 A_2 \cdots A_n}$, can be written as

$$\rho'_{A_1 A_2 \cdots A_n} = \sum_{k_1, k_2, \cdots, k_n} E_{k_1 k_2 \cdots k_n} \rho_{A_1 A_2 \cdots A_n} E_{k_1 k_2 \cdots k_n}^{\dagger}, \tag{SEQ12}$$

with $E_{k_1 k_2 \cdots k_n} = E_{k_1}^{(1)} \otimes E_{k_2}^{(2)} \otimes \cdots \otimes E_{k_n}^{(n)}$. Here, $E_{k_j}^{(j)}$, $j = 1, 2, \cdots, n$, are the Kraus operator for the local action on subsystem $A_j$ with dimension $d_j$ so that $0 \leq k_j \leq d_j^2 - 1$. Now, we describe the Kraus operators of a number of single-qubit quantum channels, namely, the amplitude- and phase-damping, and depolarizing channels [SR12, SR18].

*Amplitude-damping channel.* The AD channel represents a scenario where energy dissipation from a quantum system is allowed. The Kraus operators for a single-qubit AD channel are given by

$$E_0 = \begin{pmatrix} 1 & 0 \\ 0 & \sqrt{1-p} \end{pmatrix}, \quad E_1 = \begin{pmatrix} 0 & \sqrt{p} \\ 0 & 0 \end{pmatrix}, \tag{SEQ13}$$

with $0 \leq p \leq 1$, where $p$ corresponds to the strength of the noise acting on the input qubit state.

*Phase-damping channel.* As an example of a non-dissipative channel, we consider the PD channel. A state, after passing through the PD channel, or the "dephasing" channel, decays its off-diagonal elements, resulting in information loss about its coherence. The single qubit Kraus operators for the PD channel are given by

$$E_0 = \sqrt{1-p}I, \ E_1 = \frac{\sqrt{p}}{2}(I + \sigma_3), \ E_2 = \frac{\sqrt{p}}{2}, (I - \sigma_3), \tag{SEQ14}$$

where $I$ is the identity matrix in the qubit Hilbert space, and $p$ is again the noise-strength.

*Depolarizing channel.* In the case of the DP channel, the input qubit is depolarized, that is, replaced by the completely mixed state $\frac{I}{2}$, with probability $p$ and is left unaltered with probability $(1 - p)$. Such an operation on the single-qubit state $\rho$ is represented by

$$\rho' = \frac{p}{2}I + (1 - p)\rho. \tag{SEQ15}$$

Note that the form in Eq. (SEQ15) is not in the operator-sum representation. The operation given in Eq. (SEQ15) is often parametrized as

$$\rho' = (1 - p)\rho + \frac{p}{3}(\sigma_1 \rho \sigma_1 + \sigma_2 \rho \sigma_2 + \sigma_3 \rho \sigma_3), \tag{SEQ16}$$

leading to single qubit Kraus operators of the form given by

$$E_0 = \sqrt{1-p}I, \ E_1 = \sqrt{\frac{p}{3}}\sigma_1, \ E_2 = \sqrt{\frac{p}{3}}\sigma_2, \ E_3 = \sqrt{\frac{p}{3}}\sigma_3. \tag{SEQ17}$$

**Remark.** Similar to the case of global noise, in the case of local noisy channels also, the noiseless case is denoted by $p = 0$, while $p = 1$ represents maximal disturbance of the state.

## SSEC4. NEGATIVITY MONOGAMY SCORE UNDER DECOHERENCE

### A. Generalized GHZ state

Let us first consider the case of global noise acting on the gGHZ state. The final state, $\rho^{\text{gGHZ}}$, as a function of the mixing parameter, $p$, can be obtained following the methodology described in SSEC3, which leads to two-party reduced states $\rho_{12}^{\text{gGHZ}}$ and $\rho_{13}^{\text{gGHZ}}$ of the form $\rho_{12}^{\text{gGHZ}} = \rho_{13}^{\text{gGHZ}} = (1-p)(|a_0|^2|00\rangle\langle00| + |a_1|^2|11\rangle\langle11|) + \frac{p}{4}I$, with $I$ being a $4 \times 4$ identity matrix. They still remain classically correlated with vanishing entanglement and quantum discord. In case of AD, PD, and DP channels, the resulting states $\rho^{\text{gGHZ}}$ are obtained as (see SSEC3) $\rho^{\text{gGHZ}} = \sum_{i=0}^{1} |a_i|^2 (u_i^p|0\rangle\langle0| + v_i^p|1\rangle\langle1|)^{\otimes 3} + w^p(a_0 a_1^*|000\rangle\langle111| + h.c.)$. Here the functions $u_i^p$, $v_i^p$, and $w^p$, for the three channels, are given by

$$\begin{aligned}
\text{AD channel} &: u_i^p = \delta_{0i} + p\delta_{1i}, v_i^p = (1 - p)\delta_{1i}, w^p = (1 - p)^{\frac{3}{2}}, \\
\text{PD channel} &: u_i^p = \delta_{0i}, v_i^p = \delta_{1i}, w^p = (1 - p)^3, \\
\text{DP channel} &: u_i^p = q\delta_{0i} + (1 - q)\delta_{1i}, v_i^p = (1 - q)\delta_{0i} + q\delta_{1i}, \\
& \quad w^p = (2q - 1)^3,
\end{aligned} \tag{SEQ18}$$

with $q = 1 - \frac{2p}{3}$. From the above expressions, it can be shown that the two-qubit reduced density matrices, in case of the PD channel, do not depend on the noise parameter $p$, and remain classically correlated. On the other hand, $\rho_{12}^{\text{gGHZ}}$ and $\rho_{13}^{\text{gGHZ}}$ remains diagonal in the computational basis $\{|00\rangle, |01\rangle, |10\rangle, |11\rangle\}$, resulting in vanishing entanglement as well as quantum discord for the other two channels also. In effect, even for $p \neq 0$, $\delta_{\mathcal{N}}$ and $\delta_D$ are given by $\delta_{\mathcal{N}} = \mathcal{N}(\rho_{1:23}^{\text{gGHZ}})$ and $\delta_D = \mathcal{D}(\rho_{1:23}^{\text{gGHZ}})$ respectively, when the gGHZ state is subjected to these four types of noise. Hence, both negativity and quantum discord are always monogamous in the present

scenario, which can be applied to discriminate channels. Note that all the above discussions hold for the gGHZ state of arbitrary number of parties subjected to different types of local and global noise considered in this paper.

Using the expression for $\rho^{\text{gGHZ}}$, analytical expressions of $\delta_{\mathcal{N}}$, as functions of the noise parameter, $p$, and the state parameter, $|a_0|$, can be obtained for different types of noise. In the case of the global noise, it is given by

$$\delta_{\mathcal{N}}^g = \left| \min\left[ 0, \frac{1}{2}\left\{ \frac{p}{4} - 2|a_0||a_1|(1-p) \right\} \right] \right|, \tag{SEQ19}$$

while in the case of PD channel,

$$\delta_{\mathcal{N}}^{pd} = |a_0||a_1|(1-p)^3. \tag{SEQ20}$$

The expressions of negativity monogamy score in the case of AD channel ($\delta_{\mathcal{N}}^{ad}$) and DP channel ($\delta_{\mathcal{N}}^{dp}$) are given by

$$\delta_{\mathcal{N}}^{ad} = \left| \min\left[ 0, \frac{1}{2}\left\{ |a_1|^2 p(1-p) - \sqrt{f_1^{ad} + f_2^{ad}} \right\} \right] \right|, \tag{SEQ21}$$

$$\delta_{\mathcal{N}}^{dp} = \left| \min\left[ 0, \frac{1}{2}\left\{ q(1-q) - \sqrt{f_1^{dp} + f_2^{dp}} \right\} \right] \right|, \tag{SEQ22}$$

with the functions $f_1^{ad}$, $f_2^{ad}$, $f_1^{dp}$, and $f_2^{dp}$ defined as $f_1^{ad} = |a_1|^4(4p^6 - 12p^5 + 13p^4 - 6p^3 + p^2)$, $f_2^{ad} = 4|a_0|^2|a_1|^2(1-p)^3$, $f_1^{dp} = q^2(1-q)^2(1-2q)^2$, and $f_2^{dp} = 4|a_0|^1|a_1|^2(1-2q)^2(1-3q+3q^2)(1-5q+5q^2)$. Note here that in all the above expressions, one can replace $|a_1|$ by $\sqrt{1-|a_0|^2}$.

## B. Generalized W state

When the gW state is subjected to global noise, the evolved three-qubit state, $\rho^{\text{gW}}$ leads to the two-qubit reduced density matrix, $\rho_{12}^{\text{gW}}$, of the form $\rho_{12}^{\text{gW}} = \frac{p}{4}I_4 + (1-p)\left( |a_0|^2 P[|00\rangle] + P[|\psi\rangle] \right)$ in the computational basis, where $P[|x\rangle] = |x\rangle\langle x|$, and $|\psi\rangle = a_1|01\rangle + a_2|10\rangle$. The reduced state of qubits 1 and 3 can be determined from $\rho_{12}^{\text{gW}}$ by interchanging $a_0$ and $a_1$. One should note here that unlike the gGHZ state, the reduced states with, as well as without, noise in the current case, are no more "classical-classical" states, and possess non-vanishing entanglement as well as quantum discord. For the AD channel, the three-qubit resulting state, starting from $|\Phi\rangle$, is given by $\rho^{\text{gW}} = pP[|000\rangle] + (1-p)P[|\Phi\rangle]$, leading to $\rho_{12}^{\text{gW}} = [p + (1-p)|a_0|^2]P[|00\rangle] + (1-p)P[|\psi\rangle]$, while $\rho_{13}^{\text{gW}}$ is obtained by interchanging $a_0$ and $a_1$ in $\rho_{12}^{\text{gW}}$. In case of the PD channel, we define the states $|\tilde{\psi}\rangle = (1-p)(h_0 a_0|001\rangle + h_1 a_1|010\rangle + h_2 a_2|100\rangle)$, and $|\tilde{\phi}\rangle = h_1 a_1|01\rangle + h_2 a_2|10\rangle$, so that $h_i h_j = (1-p)^{-2}$ if $i = j$, and 1 otherwise. In terms of $|\tilde{\psi}\rangle$ and $|\tilde{\phi}\rangle$, $\rho^{\text{gW}} = P[|\tilde{\psi}\rangle]$, and $\rho_{12}^{\text{gW}} = |a_0|^2 P[|00\rangle] + (1-p)P[|\tilde{\phi}\rangle]$, respectively. Again, $\rho_{13}^{\text{gW}}$ can be obtained from $\rho_{12}^{\text{gW}}$ by interchanging $a_0$ and $a_1$. The form of $\rho^{\text{gW}}$ in the case of the DP channel is given by $\rho^{\text{gW}} = \sum_{i=1}^3 |a_{i-1}|^2 \varrho^{\otimes(i-1)} \otimes \varrho' \otimes \varrho^{\otimes(3-i)} + (2q-1)^2\left[ \left( a_0 a_1^* \varsigma_1 + a_0 a_2^* \varsigma_2 + a_1 a_2^* \varsigma_3 \right) + h.c. \right]$, where $\varrho = qP[|0\rangle] + (1-q)P[|1\rangle]$, $\varrho' = (1-q)P[|0\rangle] + qP[|1\rangle]$, with $\varsigma_1 = \varrho \otimes |0\rangle\langle 1| \otimes |1\rangle\langle 0|$, $\varsigma_2 = |0\rangle\langle 1| \otimes \varrho \otimes |1\rangle\langle 0|$, $\varsigma_3 = |0\rangle\langle 1| \otimes |1\rangle\langle 0| \otimes \varrho$. The two-qubit reduced states, $\rho_{12}^{\text{gW}}$ and $\rho_{13}^{\text{gW}}$, can be obtained from the form of $\rho^{\text{gW}}$ by tracing out qubit 3 and 2 respectively. As in the case of global noise, local density matrices, up to certain value of the noise parameter, remains quantum correlated.

In case of the global noise, negativity score, $\delta_{\mathcal{N}}^g$, is given by

$$\delta_{\mathcal{N}}^g = \left| \min\left[ 0, s^g \right] \right| - \left| \min\left[ 0, s_{12}^g \right] \right| - \left| \min\left[ 0, s_{13}^g \right] \right|, \tag{SEQ23}$$

with $s^g = \frac{p}{8} - (1-p)|a_2|\sqrt{1-|a_2|^2}$, and $s_{12}^g = \frac{1}{4}\left[ p + 2(1-p)(|a_0|^2 - \sqrt{|a_0|^4 + 4|a_1|^2|a_2|^2}) \right]$, while for the PD channel, $\delta_{\mathcal{N}}^{pd}$ is obtained as

$$\delta_{\mathcal{N}}^{pd} = s^{pd} - \frac{1}{2}\left( s_{12}^{pd} + s_{13}^{pd} + |a_2|^2 - 1 \right), \tag{SEQ24}$$

where $s^{pd} = (1-p)^2|a_2|^2([1-|a_2|^2)^{\frac{1}{2}}$, $s_{12}^{pd} = [|a_0|^2 + 4|a_1|^2|a_2|^2(1-p)^4]^{\frac{1}{2}}$. In both the cases, $s_{13}^g$ and $s_{13}^{pd}$ are obtained from $s_{12}^g$ and $s_{12}^{pd}$, respectively, by interchanging $|a_0|$ and $|a_1|$. The expressions for negativity score, $\delta_{\mathcal{N}}^{ad}$, in the case of AD channel, is given by

$$\delta_{\mathcal{N}}^{ad} = \frac{1}{2}\left[ (s^{ad} - p) - (s_{12}^{ad} - \tilde{p}_0) - (s_{13}^{ad} - \tilde{p}_1) \right], \tag{SEQ25}$$

where $s^{ad} = \sqrt{p^2 + 4(1-|a_2|^2)|a_2|^2(1-p)^2}$, and $s_{12}^{ad} = \sqrt{\tilde{p}_0^2 + 4|a_1|^2|a_2|^2(1-p)^2}$, with $\tilde{p}_j = p + (1-p)(\delta_{j0}|a_0|^2 + \delta_{j1}|a_1|^2)$. Here also, the function $s_{13}^{ad}$ is obtained from $s_{12}^{ad}$ by interchanging $a_0$ and $a_1$. The expression for $\delta_{\mathcal{N}}^{dp}$, in the case of the DP channel, can also be obtained following the same procedure as in the cases of other three types of noise. However, the expression is rather involved, and to keep the text uncluttered, we choose not to include the expression.

| Noise-types | (I) % of states $\in \mathcal{S}_x$ | | (II) % of states $\in \mathcal{S}_z$ | | (III) % of states $\notin \mathcal{S}$ | | (IV) Values of $\varepsilon_{max}$ | |
|---|---|---|---|---|---|---|---|---|
| | $\rho_{1:23}^{\text{gW}}$ | $\rho_{12}^{\text{gW}}$ | $\rho_{1:23}^{\text{gW}}$ | $\rho_{12}^{\text{gW}}$ | $\rho_{1:23}^{\text{gW}}$ | $\rho_{12}^{\text{gW}}$ | $\rho_{1:23}^{\text{gW}}$ | $\rho_{12}^{\text{gW}}$ |
| Global | $13.4 \times 10^{-2}$ | 76.632 | 99.866 | 23.367 | 0 | $1 \times 10^{-3}$ | 0 | $1.23 \times 10^{-3}$ |
| AD | 99.937 | 99.9027 | $6.3 \times 10^{-2}$ | $9.73 \times 10^{-2}$ | 0 | 0 | 0 | 0 |
| PD | $9.73 \times 10^{-2}$ | 9.617 | 99.9027 | 90.373 | 0 | $1 \times 10^{-2}$ | 0 | $2.75 \times 10^{-3}$ |
| DP | 96.479 | 95.735 | 3.521 | 4.265 | 0 | 0 | 0 | 0 |

TABLE ST1. Percentages of the states of the form $\rho^{\text{gW}}$ and $\rho_{12}^{\text{gW}}$, belonging to the sets $\mathcal{S}_x$ and $\mathcal{S}_z$, are given in the columns **(I)** and **(II)** for gW states subjected to different noise models. The fraction of states of the form $\rho^{\text{gW}}$ and $\rho_{12}^{\text{gW}}$, which do not belong to either of $\mathcal{S}_x$ or $\mathcal{S}_z$, are given in the column **(III)**. The upper bound of the absolute error, $\varepsilon_{max}$, is given in column **(IV)** for different types of noise considered in this paper. In each column, the first sub-column corresponds to the states of the form $\rho^{\text{gW}}$, while the second is for $\rho_{12}^{\text{gW}}$.

### SSEC5. COMPUTATION OF DISCORD MONOGAMY SCORE FOR GENERALIZED W STATES: NUMERICAL ANALYSIS

The computation of $\delta_{\mathcal{D}}$, in case of the gW states under noise, requires more numerical resources than that in the case of the gGHZ states, since both $\mathcal{D}\left(\rho_{12}^{\text{gW}}\right)$ and $\mathcal{D}\left(\rho_{13}^{\text{gW}}\right)$ do not vanish for almost all $p$. In the present case, $\delta_{\mathcal{D}}$ can be written as $\delta_{\mathcal{D}} = S - S(\rho_1^{\text{gW}}) - S_c$, where $S = S(\rho_{12}^{\text{gW}}) + S(\rho_{13}^{\text{gW}}) - S(\rho^{\text{gW}})$, and $S_c = S(\rho_{2|1}^{\text{gW}}) + S(\rho_{3|1}^{\text{gW}}) - S(\rho_{23|1}^{\text{gW}})$. The determination of $\delta_{\mathcal{D}}$ for a single three-qubit state requires, in principle, three separate optimizations for the terms in $S_c$. However, information acquired via numerical analysis using constrained optimization [SR9] may result in considerable reduction of the computational complexity.

Let us first concentrate on the computation of $\mathcal{D}(\rho_{1:23}^{\text{gW}})$ under four types of noise considered in this paper. We perform extensive numerical search by Haar uniformly generating a set of $3 \times 10^6$ random three-qubit states of the form $\rho'$ for each of the types of noise considered in this paper. We find that for all such states, considering two sets of values of the real parameters, $(\theta, \phi)$, in projection measurements involved in $\mathcal{D}(\rho_{1:23}^{\text{gW}})$, is enough. These sets are given by **(i)** $\theta = \pi/2, 0 \leq \phi < 2\pi$, and **(ii)** $\theta = 0, \pi, 0 \leq \phi < 2\pi$, which correspond to projection measurements on the $(x, y)$ plane, and along the $z$ axis of the Bloch sphere, respectively. Without any loss of generality, one can consider a projection measurement corresponding to the observable $\sigma_x$ in the former case, while a projection measurement corresponding to $\sigma_z$ in the latter. We refer to the set of states of the form $\rho^{\text{gW}}$, for which measurement corresponding to $\sigma_x$, or $\sigma_z$ provides the optimal measurement, as the "special" set, denoted by $\mathcal{S}$. In the present case, the set $\mathcal{S}$ represents the set of all states of the form $\rho^{\text{gW}}$, for each of the types of noise, according to our numerical analysis. The set of states for which the optimization occurs for $\sigma_x$, is denoted by $\mathcal{S}_x$, while $\mathcal{S}_z$ represents the set of $\rho^{\text{gW}}$ for which optimal measurement corresponds to $\sigma_z$. Note that $\mathcal{S} = \mathcal{S}_x \cup \mathcal{S}_z$, while $\mathcal{S}_x \cap \mathcal{S}_z = \Phi$, the null set.

The situation is a little different in the case of the two-qubit states $\rho_{12}^{\text{gW}}$ and $\rho_{13}^{\text{gW}}$, obtained from $\rho^{\text{gW}}$. We generate $3 \times 10^6$ states Haar uniformly, which are of the form $\rho_{12}^{\text{gW}}$, and we find that, like in the case of $(\rho_{1:23}^{\text{gW}})$, there exists, for each type of noise, a "special" set, $\mathcal{S}$, of states $\rho_{12}^{\text{gW}}$, for which optimization occurs corresponding to either $\sigma_x$, or $\sigma_z$. However, in the case of global noise and PD channel, a small fraction of $\rho_{12}^{\text{gW}}$ does not belong to $\mathcal{S}$, and the optimization of $\mathcal{D}(\rho_{12}^{\text{gW}})$, for these states, occur for other values of $(\theta, \phi)$. Let the maximum absolute error, resulting from the assumption that all the three-qubit states of the form $\rho_{12}^{\text{gW}}$ belong to $\mathcal{S}$, in the case of the global noise and PD channel, is $\varepsilon$. Our numerical analysis provides an upper bound of $\varepsilon$, denoted by $\varepsilon_{max}$, which is of the order of $10^{-3}$ in the case of both types of noise. Table ST1 displays our findings regarding the percentages of states of the form $\rho^{\text{gW}}$ and $\rho_{12}^{\text{gW}}$, that belong to the sets $\mathcal{S}_x$, $\mathcal{S}_z$, and do not belong to $\mathcal{S}$ for all the four types of noise. The last column (column **(IV)**) tabulates the values of $\varepsilon_{\max}$ in the relevant cases. From now on, unless otherwise mentioned, we determine the values of $\delta_{\mathcal{D}}$ by computing quantum discord with the assumption that the states either belong to $\mathcal{S}_x$ or $\mathcal{S}_z$.

### SSEC6. TYPES OF DYNAMICS WITH GENERALIZED W STATES AS INPUT

In case of the gW state subjected to global or local noise, the set of different types of dynamics that $\delta_{\mathcal{N}}$ and $\delta_{\mathcal{D}}$ undergo is far richer compared to that for gGHZ states. While only monotonic decay of $\delta_{\mathcal{N}}$ and $\delta_{\mathcal{D}}$ with increasing $p$ is found in the latter case, non-monotonic dynamics of monogamy scores emerges in the former. As an example, consider the set of gW states having a fixed value of $|a_2|$. The states in the set can be represented by the different allowed values of the absolute value of the free parameter, $a_0$. Fig. SF1 depicts the landscapes of $\delta_{\mathcal{N}}$, in the case of global noise, and of $\delta_{\mathcal{D}}$, in the case of the AD channel, as functions of $|a_0|$ and $p$, for $|a_2| = 0.7$. The solid lines in the figures represent contours obtained by joining the points having a constant value of either $\delta_{\mathcal{N}}$, or $\delta_{\mathcal{D}}$. Note that the contours form closed curves, and from outside to inside, the lines represent increasing values of $\delta_{\mathcal{N}}$ and $\delta_{\mathcal{D}}$. The dashed lines in the plots represent the dynamics of $\delta_{\mathcal{N}}$, in the case of global noise, and $\delta_{\mathcal{D}}$, in the case of the AD channel, when the input gW state is taken with $|a_0| = 0.5$. The behavior of the monogamy scores with increasing values of $p$ are non-monotonic, as clearly indicated from the values of $\delta_{\mathcal{N}}$ and $\delta_{\mathcal{D}}$, represented by different shades in Fig. SF1. An increase in the monogamy scores can be argued to be a signature of increase in quantumness. Although noise destroys quantum correlations, here we see the opposite
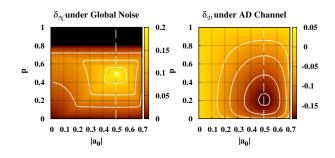
FIG. SF1. (Color online.) Variation of monogamy score corresponding to (a) $\delta_{\mathcal{N}}$ in the case of global noise, and (b) $\delta_{\mathcal{D}}$ in the case of amplitude damping channel, as functions of the state parameter $|a_0|$, and the noise parameter $p$, when gW state is subjected to noise. The value of $|a_2|$ is fixed at 0.7, while the value of $|a_1|$ is determined via normalization. The dynamics of monogamy score along the dashed line at $|a_0| = 0.5$ is non-monotonic in both the cases. The solid lines represent the contours obtained by joining the points at which $\delta_{\mathcal{N}}$, or $\delta_{\mathcal{D}}$ has a fixed value. From outside to inside, the closed contours correspond to (a) $\delta_{\mathcal{N}} = 0.05, 0.10, 0.15, 0.18$, and (b) $\delta_{\mathcal{D}} = -0.05, -0.10, -0.15, -0.18$. All the quantities plotted are dimensionless, except $\delta_{\mathcal{D}}$, which is in bits.

| Noise-types | a | | b | | c | | d | |
| --- | --- | --- | --- | --- | --- | --- | --- | --- |
| | $\delta_{\mathcal{N}}$ | $\delta_{\mathcal{D}}$ | $\delta_{\mathcal{N}}$ | $\delta_{\mathcal{D}}$ | $\delta_{\mathcal{N}}$ | $\delta_{\mathcal{D}}$ | $\delta_{\mathcal{N}}$ | $\delta_{\mathcal{D}}$ |
| Global | 75.009 | 13.330 | 0.186 | 0.003 | 24.805 | 83.536 | 0.000 | 0.131 |
| AD | 17.532 | 13.321 | 57.663 | 0.012 | 23.964 | 82.902 | 0.841 | 3.765 |
| PD | 56.145 | 13.323 | 19.050 | 0.010 | 24.784 | 53.272 | 0.021 | 33.395 |
| DP | 53.531 | 8.708 | 21.664 | 4.625 | 24.802 | 68.710 | 0.003 | 17.957 |

TABLE ST2. The percentage of gW states exhibiting **a**, **b**, **c**, and **d**-type dynamics for $\delta_{\mathcal{N}}$ and $\delta_{\mathcal{D}}$ under the application of different types of noise.

by obtaining non-monotonicity of monogamy score with the increase of $p$.

**Types of dynamics.** Now we catalog four "typical" dynamics profiles observed for both $\delta_{\mathcal{N}}$ and $\delta_{\mathcal{D}}$ for global noise as well as for AD, PD, and DP local channels. **a.** In the first profile, $\delta_{\mathcal{Q}}(p = 0) \geq 0$, and $\delta_{\mathcal{Q}}(p)$ goes to zero non-monotonically as $p \to 1$. **b.** For the second one, $\delta_{\mathcal{Q}}(p)$ monotonically goes to zero when $p$ increases, with $\delta_{\mathcal{Q}}(p = 0) \geq 0$. **c.** In contrast to the first two profiles, $\delta_{\mathcal{Q}}(p = 0) < 0$ for the third profile. With an increase of $p$, $\delta_{\mathcal{Q}}$ vanishes non-monotonically. **d.** Similar to the third profile, the fourth and final profile starts with a non-monogamous scenario ($\delta_{\mathcal{Q}}(p = 0) < 0$). However, with increasing $p$, $\delta_{\mathcal{Q}}(p)$ goes to zero monotonically as $p \to 1$.

Evidently, the frequencies of occurrence of the dynamics types **a**, **b**, **c**, and **d** must vary for different types of noise, and for different observables, viz., $\delta_{\mathcal{N}}$, and $\delta_{\mathcal{D}}$. To estimate these, we prepare a sample of $10^6$ Haar-uniformly generated gW states as input, which can be subjected to each of the types of noise, and study the dynamics profiles of the states. We find that at $p = 0$, 75.195% of the gW states are monogamous when negativity is considered, while only 13.333% of them are monogamous with respect to quantum discord. When the value of $p$ is increased, the four types of dynamics are found to occur with different frequencies in the case of the global noise and the local channels (see Table ST2). Note that for $\delta_{\mathcal{N}}$, type-**a** is more frequent in the case of global noise as well as for the PD and DP channels, while type-**b** occurs mostly in the case of the AD channel. The frequency of occurrence of **d** is much less compared to that of **a**, **b**, and **c** for the negativity monogamy score. Among all the noisy channels, the non-monotonic decay of $\delta_{\mathcal{N}}$ occurs close to 100% of times when global noise acts on the gW state, irrespective of the sign of $\delta_{\mathcal{N}}$ at $p = 0$. On the other hand, in the case of $\delta_{\mathcal{D}}$, frequency of occurrence of **c** and **d** is high in the cases of global noise and the AD channel, while the same is moderate in the case of the PD and the DP channels.

## SSEC7. DYNAMICS TERMINAL FOR GENERALIZED W STATES

To check whether the dynamics terminal, $\langle p_t \rangle$, can distinguish between different types of noise, one has to determine the value of $\langle p_t \rangle$ for different types of noise with gW states as input states, which, in turn, requires the determination of $P(p_t)$. In order to determine $P(p_t)$, we Haar uniformly generate $10^6$ gW states for each of the four kinds of noise, and study their dynamics profiles to determine $\langle p_t \rangle$. The variations of $P(p_t)$ against $p_t$ are given in Fig. SF2. It is clear from the figure that the maximum possible value of $p_t$ is considerably different in the case of $\delta_{\mathcal{N}}$ and $\delta_{\mathcal{D}}$, when the type of noise is fixed. The values of $\langle p_t \rangle$ corresponding to $\delta_{\mathcal{N}}$ and $\delta_{\mathcal{D}}$, for global noise, AD channel, PD channel, and DP channel are given in Table I. Note that the dynamics terminal corresponding to $\delta_{\mathcal{D}}$ is higher than that corresponding to $\delta_{\mathcal{N}}$ in the case of the global noise, AD channel, and the DP channel, while the trend is reversed in the case of the PD channel.
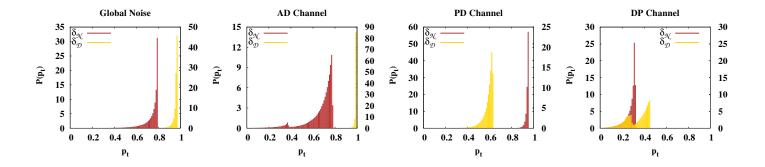
FIG. SF2. (Color online.) Variations of the normalized probability density function, $P(p_t)$, against the dynamics terminal, $p_t$, for $\delta_{\mathcal{N}}$ and $\delta_{\mathcal{D}}$, when gW states are subjected to different types of noise. All quantities plotted are dimensionless.
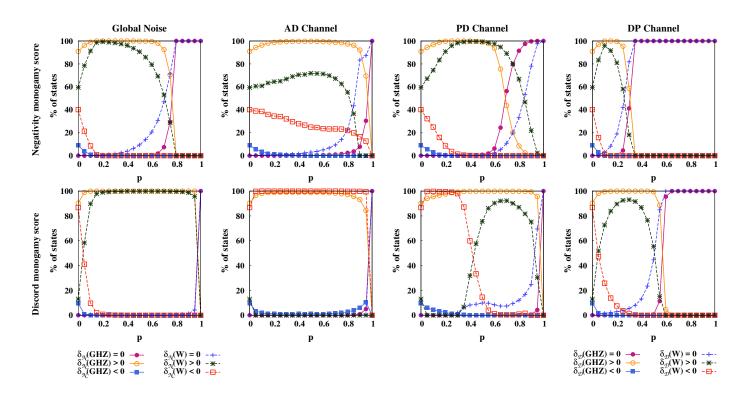


FIG. SF3. (Color online.) Variations of the percentages of arbitrary three-qubit pure states chosen from GHZ class (continuous lines) and W class (broken lines), for which monogamy scores corresponding to negativity and quantum discord are strictly greater than, equal to, and strictly less than zero (denoted by different types of points), with the noise parameter, $p$. All quantities plotted are dimensionless.

## SSEC8. DYNAMICS OF MONOGAMY SCORE IN ARBITRARY TRIPARTITE PURE STATES

Hitherto, we have investigated gGHZ and gW states, for which the effects of various noisy channels on monogamy scores can be addressed analytically up to certain extent. To complete the investigation for three-qubit states as input, we now consider the two mutually exclusive and exhaustive classes of three-qubit states, viz., the GHZ class and the W class [SR19]. These two classes, inequivalent under stochastic local operations and classical communication (SLOCC), together span the entire set of three-qubit pure states [SR19]. An arbitrary three-qubit pure state from the GHZ class, up to local unitary operations, can be parametrized as $|\psi_{GHZ}\rangle = \sqrt{K}(c_\delta|000\rangle + s_\delta e^{i\varphi}|\varphi_\alpha\rangle|\varphi_\beta\rangle|\varphi_\gamma\rangle)$, where $|\varphi_k\rangle = c_k|0\rangle + s_k|1\rangle$ with $c_k = \cos k$, $s_k = \sin k$, $k = \alpha, \beta, \gamma$, and $K = (1 + 2c_\delta s_\delta c_\alpha c_\beta c_\gamma c_\varphi)^{-1} \in (\frac{1}{2}, \infty)$ is the normalization factor. Here, the ranges for the five real parameters are $\delta \in (0, \pi/4], \alpha, \beta, \gamma \in (0, \pi/2]$ and $\varphi \in [0, 2\pi)$. On the other hand, a three-qubit pure state from the W class, up to local unitaries, can be written in terms of three real parameters as $|\psi_W\rangle = \sqrt{a}|001\rangle + \sqrt{b}|010\rangle + \sqrt{c}|100\rangle + \sqrt{1 - (a + b + c)}|000\rangle$, where $a, b, c \geq 0$.
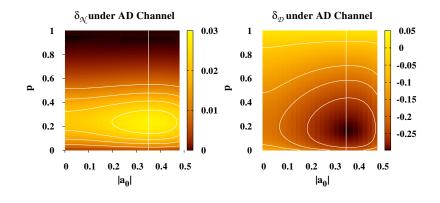
FIG. SF4. (Color online.) Variation of monogamy scores corresponding to (a) $\delta_{\mathcal{N}}$ and (b) $\delta_{\mathcal{D}}$ in the case of the amplitude damping channel, as functions of the state parameter $|a_0|$, and the noise parameter $p$, when the four-qubit gW state is subjected to the noise. The value of $|a_2|$ and $|a_3|$ are fixed at 0.5 and 0.7, respectively, while the value of $|a_1|$ is determined via normalization. The dynamics of monogamy scores along the thick solid lines at $|a_0| = 0.35$ are non-monotonic in both the cases. The thin dashed lines represent the contours obtained by joining the points at which $\delta_{\mathcal{N}}$, or $\delta_{\mathcal{D}}$ have a fixed value. From outside to inside, the closed contours correspond to (a) $\delta_{\mathcal{N}} = 0.01, 0.015, 0.02, 0.025$, and (b) $\delta_{\mathcal{D}} = -0.05, -0.15, -0.2, -0.25$. All the quantities plotted are dimensionless, except $\delta_{\mathcal{D}}$, which is in bits.

Due to higher number of state parameters in arbitrary three-qubit pure states chosen from these classes, determining compact forms for $\delta_{\mathcal{N}}$ as well as $\delta_{\mathcal{D}}$ is difficult. Also, the constrained optimization is not applicable due to the high absolute error in the value of quantum discord. Therefore, we employ exact numerical optimization technique to compute quantum discord in discord monogamy scores of these states. We Haar-uniformly generate $10^4$ states from each of the two classes – the GHZ class and the W class – for a chosen value of the noise parameter, $p$, when a specific type of noise is applied to it. We then determine the percentage of states for which negativity and discord monogamy scores are greater than, equal to, and less than zero, and study the variation of these percentages with varying noise parameter.

The variation of the percentages of three-qubit pure states from the GHZ and W classes, for which $\delta_{\mathcal{N}}$ and $\delta_{\mathcal{D}}$ are >, =, and < 0, against $p$ is given in Fig. SF3. The percentages vary non-monotonically with varying noise parameter, and the percentage of states for which the monogamy scores corresponding to negativity and quantum discord are equal to zero, for both classes of states, tend to become 100% with increasing $p$, as expected. For both the classes, this trend is considerably slower in the case of global noise, AD channel, and PD channel, in comparison to that for the DP channel. The patterns in the W class states are similar to those in the case of gW states, except for discord monogamy score under PD channel. While no gW states have a strictly positive $\delta_{\mathcal{D}}$ for higher values of $p$, in the case of W class states, the corresponding fraction increases with increasing $p$, reaches a maximum value at moderately high $p$, and then, as expected, decreases to zero as $p \to 1$.

## SSEC9.  DYNAMICS OF MONOGAMY SCORE FOR HIGHER NUMBER OF PARTIES

The question that naturally arises from the results reported in the preceeding sections is whether the dynamical features found in the case of three-qubit systems is generic for quantum states with higher number of qubits. As we have already mentioned, the monogamy score of gGHZ state decreases monotonically with the increase of $p$ for an arbitrary number of parties. And, the non-monotonic behaviour of the monogamy scores corresponding to both negativity and quantum discord, in the case of the three-qubit generalized W state under, for example, the AD channel, is found in the case of higher number of qubits. This can be clearly seen in Fig. SF4, where the variations of $\delta_{\mathcal{N}}$ and $\delta_{\mathcal{D}}$, in the case of the four-qubit generalized W state $|\Phi_4\rangle = a_0|0001\rangle + a_1|0010\rangle + a_2|0100\rangle + a_3|1000\rangle$, is depicted as functions of the noise parameter $p$, and the state parameter, $|a_0|$. We fix $|a_3| = 0.7$ and $|a_2| = 0.5$ for demonstration, where $|a_1|$ is fixed by normalization. We also find that similar to the three-qubit scenario, the depolarizing channel destroys the monogamy scores corresponding to both negativity and quantum discord more rapidly compared to other channels, for four qubits. We therefore expect that the broad qualitative features of the results found in the case of three qubits remain unaltered when the number of qubits is increased.

---

[SR1]  J. Lee, M. S. Kim, Y. J. Park, and S. Lee, J. Mod. Opt. **47**, 2151 (2000); G. Vidal and R.F. Werner, Phys. Rev. A **65**, 032314 (2002); M. B. Plenio, Phys. Rev. Lett. **95**, 090503 (2005).
[SR2]  A. Peres, Phys. Rev. Lett. **77**, 1413 (1996); M. Horodecki, P. Horodecki, and R. Horodecki, Phys. Lett. A **223**, 1 (1996).
[SR3]  L. Henderson and V. Vedral, J. Phys. A: Math. Gen. **34**, 6899 (2001); H. Ollivier and W. H. Zurek, Phys. Rev. Lett. **88**, 017901 (2001).

[SR4] W. H. Zurek, in Quantum Optics, Experimental Gravitation and Measurement Theory, edited by P. Meystre and M. O. Scully (Plenum, New York, 1983); S. M. Barnett and S. J. D. Phoenix, Phys. Rev. A **40**, 2404 (1989). B. Schumacher and M. A. Nielsen, Phys. Rev. A **54**, 2629 (1996); N. J. Cerf and C. Adami, Phys. Rev. Lett. **79**, 5194 (1997); B. Groisman, S. Popescu, and A. Winter, Phys. Rev. A **72**, 032317 (2005).

[SR5] Y. Huang, New. J. Phys. **16** (3), 033027 (2014).

[SR6] M. Koashi and A. Winter, Phys. Rev. A **69**, 022309 (2004).

[SR7] S. Luo, Phys. Rev. A **77**, 042303 (2008).

[SR8] M. Ali, A. R. P. Rau, and G. Alber, Phys. Rev. A **81**, 042105 (2010); *ibid.* **82**, 069902(E) (2010); X.-M. Lu, J. Ma, Z. Xi, and X. Wang, Phys. Rev. A **83**, 012327 (2011); D. Girolami and G. Adesso, Phys. Rev. A **83**, 052108 (2011); Q. Chen, C. Zhang, S. Yu, X. X. Yi, and C. H. Oh, Phys. Rev. A **84**, 042313 (2011).

[SR9] F. F. Fanchini, T. Werlang, C. A. Brasil, L. G. E. Arruda, and A. O. Caldeira, Phys. Rev. A **81**, 052107 (2010); B. Li, Z. -X. Wang, and S. -M. Fei, Phys. Rev. A **83**, 022321 (2011). Y. Huang, Phys. Rev. A **88**, 014302 (2013); M. Namkung, J. Chang, J. Shin, and Y. Kwon, arXiv: 1404.6329 [quant-ph] (2014); T. Chanda, A. K. Pal, A. Biswas, A. Sen(De), and U. Sen, Phys. Rev. A **91**, 062119 (2015); T. Chanda, T. Das, D. Sadhukhan, A. K. Pal, A. Sen(De), and U. Sen, Phys. Rev. A **92**, 062301 (2015).

[SR10] V. Coffman, J. Kundu, and W. K. Wootters, Phys. Rev. A **61**, 052306 (2000); B. Terhal, IBM J. Res. Dev. **48**, 71 (2004).

[SR11] R. Prabhu, A. K. Pati, A. Sen(De), and U. Sen, Phys. Rev. A **86**, 052337 (2012).

[SR12] J. Maziero, T. Werlang, F. F. fanchini, L. C. Céleri, and R. M. Serra, Phys. Rev. A **81**, 022116 (2010).

[SR13] Á. Rivas and S. F. Huelga, Open Quantum Systems : An Introduction (Springer Briefs in Physics, 2012); Á. Rivas, S. F. Huelga, and M. B. Plenio, Rep. Prog. Phys. **77**, 094001 (2014).

[SR14] E. C. G. Sudarshan, P. M. Mathews, and J. Rau, Phys. Rev. **121**, 920 (1961).

[SR15] K. Kraus, Ann. Phys., **64**, 311, (1971).

[SR16] M. Choi, Linear Algebra and Its Applications **10**, 285 (1975).

[SR17] K. Kraus, *States, Effects and Operations: Fundamental Notions of Quantum Theory*, Lecture Notes in Physics, Vol. **190**, Springer-Verlag, Berlin, 1983.

[SR18] J. Preskill, *Quantum Information and Computation*, Lect. Notes available at http://www.theory.caltech.edu/ people/preskill/ph229/#lecture.

[SR19] W. Dür, G. Vidal, J. I. Cirac, Phys. Rev. A **62**, 062314 (2000).